Master's thesis
Theoretical and computational methods

DARK MATTER VIA KINETIC MIXING

Sebastian Sassi
2019

Advisor: Kimmo Tuominen
Examiners: Kari Rummukainen
Matti Heikinheimo

UNIVERSITY OF HELSINKI
DEPARTMENT OF PHYSICS

PL 64 (Gustaf Hällströmin katu 2)
00014 Helsingin yliopisto

HELSINGIN YLIOPISTO
HELSINGFORS UNIVERSITET
UNIVERSITY OF HELSINKI

MATEMAATTIS-LUONNONTIETEELLINEN TIEDEKUNTA
MATEMATISK-NATURVETENSKAPLIGA FAKULTETEN
FACULTY OF SCIENCE

Tiedekunta — Fakultet — Faculty	Koulutusohjelma — Utbildningsprogram — Degree programme	
Faculty of Science	Theoretical and computational methods	
Tekijä — Författare — Author		
Sebastian Sassi		
Työn nimi — Arbetets titel — Title		
Dark matter via kinetic mixing		
Työn laji — Arbetets art — Level	Aika — Datum — Month and year	Sivumäärä — Sidoantal — Number of pages
Master's thesis	March 2019	57

Tiivistelmä — Referat — Abstract

When the standard model gauge group SU(3) × SU(2) × U(1) is extended with an extra U(1) symmetry, the resulting Abelian U(1) × U(1) symmetry introduces a new kinetic mixing term into the Lagrangian. Such double U(1) symmetries appear in various extensions of the standard model and have therefore long been of interest in theoretical physics. Recently this kinetic mixing has received attention as a model for dark matter. In this thesis, a systematic review of kinetic mixing and its physical implications is given, some of the dark matter candidates relying on kinetic mixing are considered, and experimental bounds for kinetic mixing dark matter are discussed. In particular, the process of diagonalizing the kinetic and mass terms of the Lagrangian with a suitable basis choice is discussed. A rotational ambiquity arises in the basis choice when both U(1) fields are massless, and it is shown how this can be addressed. BBN bounds for a model with a fermion in the dark sector are also given based on the most recent value of the effective number of neutrino species N_ν, and it is found that a significant portion of the FIMP regime is excluded by this constraint.

Avainsanat — Nyckelord — Keywords

dark matter, kinetic mixing, FIMP, dark photon

Säilytyspaikka — Förvaringställe — Where deposited

Muita tietoja — Övriga uppgifter — Additional information

CONTENTS

1 INTRODUCTION

The nature of dark matter is one of the great puzzles of modern physics. Evidence of its existence is substantial. The cold dark matter (CDM) paradigm accurately describes a number of cosmological and astrophysical observations that other models fail to explain those phenomena as satisfactorily. This has made the physics community quite confident that there is an unknown, undetected species of massive particle out there that interacts very little with ordinary matter. However, little more can be said about its structure with certainty. Early models of dark matter were largely motivated by the WIMP miracle*, called such because the predicted abundance of a weakly coupled particle in the electroweak mass range coincided with the observed present day abundance of dark matter, and such particles were predicted by at the time attractive supersymmetric extensions of the standard model (Jungman, Kamionkowski, and Griest 1996). Decades after the first suggestions to explain the abundance of dark matter by weakly interacting massive particles (Gunn et al. 1978), no WIMP has been detected directly or indirectly to this day despite various searches.

The failure to find a WIMP has compelled physicists to find alternative models for dark matter. Problems with the collisionless CDM model, such as inconsistencies between the predicted and observed density profiles of galactic dark matter halos (de Blok 2010), have motivated more complicated dark matter models with self interactions or richer structure in the dark sector, and models with much weaker couplings to the standard model than the typical WIMP have gained increased attention. This widening on scope has led to an increasing number of dark matter candidates to comb through.

One of the possibilities is a new dark gauge field. Although no obstruction exists in principle to piling more complex gauge groups on top of the standard model with very weak couplings to standard model particles, the simplest possibility is the introduction of an extra U(1) field X, which as an Abelian gauge field has the unique property that it can couple to the existing U(1) weak hypercharge field via a kinetic mixing term $\frac{1}{2}\varepsilon B^{\mu\nu}X_{\mu\nu}$. The extra U(1) field goes by many names, but for this thesis we will identify it as a dark photon due to its obvious similarity to the electromagnetic field when it is massless. Models with kinetic mixing have historically been motivated by grand unified theories, with extra U(1) fields arising from the breaking of larger gauge symmetries. Although kinetic mixing as a dark matter candidate appeared very early on (Goldberg and Hall 1986), only in recent years has it gained significant traction as a model for dark matter (Cheung and Yuan 2007; Feldman, Liu, and Nath 2007; Pospelov, Ritz, and Voloshin 2008; Huh et al.

*WIMP: weakly interacting massive particle

2008). There are a number of ways to get dark matter out of a model with kinetic mixing. Perhaps most importantly from the perspective of building the model, the dark photon can either be massless or massive. If it is massive but very light so as to not decay too fast, it can serve as a dark matter particle by itself (Fradette et al. 2014). Generally it is taken to come with at least a dark fermion—i.e., a fermion which only couples to the dark photon (Huh et al. 2008; Chun, Park, and Scopel 2011; Vogel and Redondo 2014). However, models with more structure with multiple fermions and bound states have also gained attention since they can resolve some issues with dark matter at galactic scales (Kaplan et al. 2010; Cyr-Racine and Sigurdson 2013; Cline et al. 2014).

The purpose of this thesis is to review kinetic mixing dark matter in its various forms, carefully examine some theoretical aspects of the models, and discuss some of the experimental and observational constraints that can be placed on various forms of kinetic mixing. In order to maintain some scope, we restrict the discussion to models with at most a single dark fermion and leave out the complexities of bound states. Much of the discussion goes through for an arbitrary amount of fermions in the dark sector, since this thesis is primarily centered around the behavior of the dark photons and less attention is given to what the fermions are doing. It is also worth noting that even though we are dealing with only one extra U(1) field, the main field theoretic results have straightforward generalizations to multiple extra U(1) fields if one chooses to go in that direction.

Chapter 2 begins with brief review of the relevant cosmology and thermodynamics and introduces the notation and formulae needed for discussing the cosmological implications of dark matter. In chapter 3 we have a general overview of dark matter. This includes a short discussion of its history from the discovery of its gravitational effects to the present paradigm of CDM as an undetected elementary particle, a discussion of modern attempts at direct detection, as well as a review of dark matter creation mechanisms. Chapter 4 gets to the main topic of the thesis and introduces the kinetic mixing Lagrangian. We diagonalize the Lagrangian into a canonical form where the kinetic mixing term vanishes, the mass matrix is diagonal, and the mixing parameter is absorbed into the physical masses and couplings of the fields. Special attention is paid to what are the physical parameters of the theory, in particular in the massless case where an extra O(2) degree of freedom in the diagonalization of the mass matrix leaves an ambiguity in the choice of basis for the fields, which turns out to have no physically observable consequences when care is taken in determining the observables. Finally, in chapter 5 we shall review some constraints on kinetic mixing dark matter, including particle physics, direct detection, astrophysical, and cosmological constraints. We also derive a bound for a BBN constraint from the effective number of neutrino species.

2 BACKGROUND

The goal of this chapter is to review some of the basic concepts in standard cosmology and thermodynamics for use later in the thesis. We will briefly discuss the dynamics of expanding spacetime in a homogeneous and isotropic universe and introduce the standard quantities used for describing thermodynamics in the early universe. In particular, we will derive the general relativistic form of the Boltzmann equation which plays a fundamental role in describing the evolution of the abundance of particle species in the universe. A standard reference to these topics is *The early universe* by Kolb and Turner (1990). See also the article of Gondolo and Gelmini (1991) on computation of cosmic relic abundances.

2.1 The FLRW universe

The universe today is known to be homogeneous and isotropic at large scales, and therefore to first order the geometry of spacetime is described by the Friedmann–Lemaître–Robertson–Walker (FLRW) metric given by

$$ds^2 = -dt^2 + a(t)^2 \left(\frac{dr^2}{1 - Kr^2} + r^2 \, d\Omega^2 \right).$$

Here K characterizes the spatial curvature while $a(t)$ is the scale factor the dynamics of which are governed by the Einstein field equations $G_{\mu\nu} + \Lambda g_{\mu\nu} = 8\pi G T_{\mu\nu}$. The matter, which is assumed to be homogeneously and isotropically distributed enters through the stress–energy tensor $T^{\mu}{}_{\nu} = (\rho + p)u^{\mu}u_{\nu} + p\delta^{\mu}{}_{\nu}$, with ρ the energy density and p the pressure of the matter. Modern cosmological observations suggest a very flat universe, which means that we can to a great approximation take $K = 0$. The field equations then lead to the Friedmann equations

$$H^2 = \frac{8\pi G\rho}{3}, \quad H^2 + \dot{H} = -4\pi G(p + \tfrac{1}{3}\rho), \tag{2.1}$$

where $H = \dot{a}/a$ is the Hubble parameter.

The Friedmann equations can be combined to give $\dot{\rho} + 3H(\rho + p) = 0$, which together with an equation of state $p = w\rho$ leads to the useful general solution $\rho \propto a^{-3(1+w)}$, where in particular we have for radiation ($w = 1/3$) that $\rho \propto a^{-4}$. The analysis done in this thesis will take place at times where the energy density of the universe was dominated by radiation, which means that the energy density $\rho \propto a^{-4}$ to a very good approximation. In this case, the Friedmann equations give $a \propto t^{1/2}$. Then the Hubble parameter takes the form $H = 1/2t$.

2.2 Thermodynamics of relativistic particles

In classical statistical mechanics the thermal distribution of particles is described by the phase space distribution $f(\boldsymbol{x}, \boldsymbol{p}, t)$, which is proportional to the likelihood of finding a particle in a phase space volume element $d^3x\, d^3p$ at time t, defined such that the number of particles in the volume element is given by $dN = f\, d^3x\, d^3p$. Relativistically we regard f also as a function of energy such that it is a function of the spacetime position x^μ and four-momentum p^μ, with the additional condition $g_{\mu\nu}p^\mu p^\nu = m^2$ to ensure that the trajectories of the particles are timelike (or lightlike in case of massless particles). For a particle species i the number density, energy density, and pressure are respectively given by

$$n_i = \frac{g_i}{(2\pi)^3} \int f_i(\boldsymbol{x}, \boldsymbol{p}, t)\, d^3p, \tag{2.2}$$

$$\rho_i = \frac{g_i}{(2\pi)^3} \int E_i f_i(\boldsymbol{x}, \boldsymbol{p}, t)\, d^3p, \tag{2.3}$$

$$p_i = \frac{g_i}{(2\pi)^3} \int \frac{p^2}{3E_i} f_i(\boldsymbol{x}, \boldsymbol{p}, t)\, d^3p, \tag{2.4}$$

where $g_i/(2\pi)^3$ is the phase space density of states with g_i being the number of internal degrees of freedom of the particle species.

For a particle species in thermodynamic equilibrium the distribution function f only depends on the energy and has the form

$$f(E) = \frac{1}{e^{(E-\mu)/T} \pm 1},$$

where the plus sign holds for fermions, and the minus sign holds for bosons, μ is the chemical potential, and T the temperature of the system. In the early universe it is often suitable to assume the chemical potential to be small compared to the temperature, so from here on we take $\mu = 0$. In this case, the entropy density s can be obtained from

$$s = \frac{\rho + p}{T}.$$

A useful limit often used in this thesis is the ultrarelativistic one, where $T \gg m$. In this limit we have

$$n_i = \frac{2g_i}{(2\pi)^2} \int_0^\infty \frac{p^2}{e^{p/T} \pm 1}\, dp = \begin{Bmatrix} 3/4 \\ 1 \end{Bmatrix} \frac{\zeta(3)}{\pi^2} g_i T^3, \tag{2.5}$$

$$\rho_i = \frac{g_i}{(2\pi)^3} \int_0^\infty \frac{p^3}{e^{p/T} \pm 1}\, dp = \begin{Bmatrix} 7/8 \\ 1 \end{Bmatrix} \frac{\pi^2}{30} g_i T^4, \tag{2.6}$$

$$p_i = \frac{\rho_i}{3}, \tag{2.7}$$

$$s_i = \begin{Bmatrix} 7/8 \\ 1 \end{Bmatrix} \frac{2\pi^2}{45} g_i T^3 \tag{2.8}$$

where the upper number in the curly brackets holds for fermions while the lower holds for bosons. We will define the effective number of relativistic degrees of freedom $g_*(T)$ from the total energy density $\rho = \sum_i \rho_i$ by

$$\rho \equiv \frac{\pi^2}{30} g_*(T) T^4. \tag{2.9}$$

Similarly we define the effective number of relativistic entropy degrees of freedom g_{*S} by

$$s \equiv \frac{2\pi^2}{45} g_{*S}(T) T^3.$$

The motivation for these definitions is clear when one considers the case where all particle species are relativistic, so that $g_* = \sum_i g_i$, and similarly for g_{*S}. It turns out that $g_* \approx g_{*S}$ to a very good approximation throughout most of the early history of the universe, which often lets us interchange these two quantities. The expression for the Hubble parameter in terms of energy density in (2.1) and equation (2.9) lead to a useful relation between time and temperature in a radiation dominated universe,

$$\frac{1}{2t} = H = \sqrt{\frac{\pi^2}{90} g_*} \frac{T^2}{M_{\mathrm{Pl}}},$$

where $M_{\mathrm{Pl}} = 1/8\pi G$ is the Planck mass.

2.2.1 The Boltzmann equation

Although a thermal equilibrium is for the most part a very good approximation for the early universe, a great deal of physical insight is also contained in the nonequilibrium thermodynamics. Therefore we would like to know the general evolution of the density function f. Since a particle's position and four-momentum uniquely define a geodesic on the spacetime manifold M, it follows that every point on the tangent bundle TM uniquely determines a path on the spacetime. These paths then define a flow according to which a distribution of noninteracting particles evolves. We can denote the vector field that generates this flow by X. Then the evolution of a general distribution f of interacting particles evolves according to the equation

$$Xf = C[f, f_i],$$

where the left hand side accounts for the geodesic flow of particles, while the right hand side accounts for their collisions, with f the distribution of the given particle species, and f_i the distributions of other particle species with which it might interact. The collision term roughly corresponds to the probability of finding a scattered particle in a given phase space element, and thus consistso of an integration over the momenta p_i of the squared scattering amplitude $|\mathcal{M}|^2$ mutliplied by products of distribution functions. We will not need the general form of $C[f, f_i]$, but a related term for the special case of two-to-two scattering is given in equation (2.15), and the form for n-to-m

scattering is a straightforward generalization of that. If we parametrize the paths by τ then X can be written in coordinate form as

$$X = \frac{\partial}{\partial \tau} = \dot{x}^\mu \frac{\partial}{\partial x^\mu} + \dot{p}^\mu \frac{\partial}{\partial p^\mu}.$$

Since p^μ satisfies the geodesic equation, we can write $\dot{p}^\mu = -\Gamma^\mu{}_{\nu\rho} p^\nu p^\rho / m$ with $\dot{x}^\mu = p^\mu / m$ This leads to the relativistic Boltzmann equation

$$p^\mu \frac{\partial f}{\partial x^\mu} - \Gamma^\mu{}_{\nu\rho} p^\nu p^\rho \frac{\partial f}{\partial p^\mu} = C[f, f_i].$$

In the FLRW metric this reduces to

$$\frac{\partial f}{\partial t} - H \frac{p^2}{E} \frac{\partial f}{\partial E} = C[f, f_i]. \tag{2.10}$$

From the Boltzmann equation, one can derive the evolution equations for the number density, energy density, and pressure by taking suitable integrals of (2.10). To obtain the evolution of the number density, we integrate (2.10) over the momenta, which leads to the equation

$$\dot{n} + 3Hn = \frac{g}{(2\pi)^3} \int C[f, f_i] \, d^3p. \tag{2.11}$$

For purposes of computation, the number density is often normalized by the entropy density s to produce the dimensionless quantity $Y = n/s$, which simplifies the equation for the abundance to

$$s\dot{Y} = \frac{g}{(2\pi)^3} \int C[f, f_i] \, d^3p. \tag{2.12}$$

The energy density is equally straightforward to obtain. Multiplying by the energy and integrating over the momenta leads to

$$\dot{\rho} + 3H(\rho + p) = \frac{g}{(2\pi)^3} \int EC[f, f_i] \, d^3p. \tag{2.13}$$

Note that for massless particles with $p = \rho/3$ this reduces to

$$\dot{\rho} + 4H\rho = \frac{g}{(2\pi)^3} \int EC[f, f_i] \, d^3p. \tag{2.14}$$

Note that equations (2.10)–(2.14) are all referred to as Boltzmann equations.

When it comes to the collision term, in this thesis we are primarily interested in two-to-two type processes, so we will only consider the expression for these processes. The general expression for an arbitrary process is a straightforward generalization of that. Rather than writing down the collision term $C[f, f_i]$ that appears in the Boltzmann equation (2.10), we just write down the form of it that has been integrated over the momenta,

$$c = \frac{g}{(2\pi)^3} \int C[f, f_i] \, d^3p.$$

Given a process $12 \to 34$, the collision term c has the form

$$\begin{aligned} -\frac{1}{S}\int [\{\mathcal{M}(12 \to 34)\}^2 f_1 f_2 (1 \pm f_3)(1 \pm f_4) - \\ \{\mathcal{M}(34 \to 12)\}^2 f_3 f_4 (1 \pm f_1)(1 \pm f_2)] \times \\ (2\pi)^4 \delta^4(p_1 + p_2 - p_3 - p_4)\, d\Pi_1\, d\Pi_2\, d\Pi_3\, d\Pi_4. \end{aligned} \tag{2.15}$$

Here $d\Pi_i = d^3p_i/(2\pi)^3 2E_i$ is the relativistically invariant phase space measure, S is a symmetry factor taking into account identical particles in the initial or final state, the curly brackets denote spin-summed squares of the quantum mechanical scattering amplitude ($\{\mathcal{M}\}^2 = \sum_{\text{all spins}} |\mathcal{M}|^2$), f_i is the distribution function for the given particle type with the $\pm$ for bosons and fermions respectively, and $\delta^4(\cdot)$ is the four dimensional delta function.

A couple of approximations can usually be made to simplify the above expression for the collision term. First, most natural processes respect time reversal symmetry to very good approximation since its violation is equivalent to CP-violation which only occurs very weakly in the standard model. For practical purposes we can therefore take $\{\mathcal{M}(12 \to 34)\}^2 = \{\mathcal{M}(34 \to 12)\}^2$. Secondly, the factors $1 \pm f$ can usually be neglected and set to unity since the occupation numbers of particles in the final state are assumed to be small. Under these assumptions we have the simpler expression

$$c = -\frac{1}{S}\int \{\mathcal{M}\}^2 [f_1 f_2 - f_3 f_4] (2\pi)^4 \delta^4(p_1 + p_2 - p_3 - p_4)\, d\Pi_1\, d\Pi_2\, d\Pi_3\, d\Pi_4,$$

where now $\{\mathcal{M}\}^2 = \{\mathcal{M}(12 \to 34)\}^2 = \{\mathcal{M}(34 \to 12)\}^2$. A further assumption that is often made is that the outgoing particles fall fast enough to thermal equilibrium that f_3 and f_4 can be approximated by their equilibrium distributions $\hat{f}_3$ and $\hat{f}_4$. The principle of detailed balance then leads to the identification $\hat{f}_3 \hat{f}_4 = \hat{f}_1 \hat{f}_2$.

The above identification implies that the distribution part $f_1 f_2 - f_3 f_4$ of the collision term can be regarded as independent of the momenta p_3 and p_4. For this reason, for two-to-two processes it is useful to write the collision term in terms of the relativistically invariant cross section σ defined by

$$\sigma = \frac{1}{F g_1 g_2}\int \{\mathcal{M}\}^2 (2\pi)^4 \delta^4(p_1 + p_2 - p_3 - p_4)\, d\Pi_3\, d\Pi_4, \tag{2.16}$$

where $F = ((p_1 \cdot p_2)^2 - m_1^2 m_2^2)^{1/2}$, and g_1 and g_2 are the numbers of spin degrees of freedom of the respective particles. In this case the collision term takes the form

$$c = -\frac{g_1 g_2}{S}\int \sigma v [f_1 f_2 - \hat{f}_1 \hat{f}_2] \frac{d^3p_1}{(2\pi)^3}\frac{d^3p_2}{(2\pi)^3},$$

where $v = F/E_1 E_2$ is known as the Møller velocity.

The presence of the Møller velocity is important in the computation of thermally averaged cross sections. The Møller velocity coincides with the relative velocity $v_{\text{rel}} = |\boldsymbol{v}_1 - \boldsymbol{v}_2|$ in the lab frame and the center of mass frame,

but is in general not the same. The equality holds whenever $\boldsymbol{v}_1$ and $\boldsymbol{v}_2$ remain parallel. This is generally not the case for a collision in a frame where the particle gas has no center of mass momentum.

The final often made assumption about the distributions is that particles 1 and 2 are in kinetic equilibrium, which means that the shape of their distribution is proportional to the equilibrium distribution; that is $f(t, E) \propto \hat{f}(E)$ for any given time t. A straightforward computation under this assumption shows that

$$c = -\frac{1}{S}\langle\sigma v\rangle(n_1 n_2 - \hat{n}_1\hat{n}_2), \tag{2.17}$$

where $\hat{n}_i$ is the equilibrium number density, and

$$\langle\sigma v\rangle = \frac{1}{\hat{n}_1\hat{n}_2}\int(\sigma v)(p_1, p_2)\frac{d^3p_1}{(2\pi)^3}\frac{d^3p_2}{(2\pi)^3}$$

is the thermal average of $\langle\sigma v\rangle$. For a particle that primarily interacts via a single two-to-two scattering process, this allows writing the Boltzmann equation as

$$\dot{n}_1 + 3Hn_1 = -\frac{1}{S}\langle\sigma v\rangle(n_1 n_2 - \hat{n}_1\hat{n}_2). \tag{2.18}$$

Under the assumption that particles 1 and 2 are identical, this reduces to the expression

$$\dot{n} + 3Hn = -\langle\sigma v\rangle(n^2 - \hat{n}^2).$$

This equation often functions as a basis for simple estimates of dark matter density in the freeze out scenario of dark matter creation.

3 DARK MATTER

Although the idea of matter not visible to our instruments has appeared in various scientific contexts throughout the history, as discussed in the historical review of Bertone and Hooper (2016), the start of the era of dark matter as an essential part of astronomy and cosmology is usually associated with the seminal research of Rubin and Ford on the rotation velocity curves of galaxies in the 1970's (Rubin and Ford 1970; Rubin, Ford, and Thonnard 1980). Since galaxies can be regarded as gravitationally bound clouds of gas, their rotation velocities can be determined in terms of their mass distributions, and conversely their mass distributions may be determined from rotation velocities. Observations of rotation velocities of galaxies throughout the 1970's led to the conclusion that a significant portion of the mass of the galaxies is contained outside the visible part of the galaxy (Roberts and Rots 1973; Einasto, Kaasik, and Saar 1974).

While the presence of nonluminous mass surrounding a galaxy is a straightforward conclusion to explain the velocity curves, it is not the only model that can explain these observations. The natural alternative to dark matter that came soon after the initial discoveries of the 1970's is that gravitational interaction itself is fundamentally modified at very small accelerations, such as the theory of modified Newtonian dynamics (MOND) suggested by Milgrom (1983) shortly after the wave of galaxy rotation studies in the 1970's. However, any complete modified theory of gravity would also have to be compatible with general relativity, which makes the construction viable theories significantly harder than the relatively simple dark matter hypothesis.

In addition to the theoretical difficulties associated with theories of modified gravity that can explain the galaxy rotation curves, from the 1980's onwards further observations strengthened the dark matter hypothesis. One line of observations coming from galaxy clusters provides two independent pieces of evidence for dark matter. On one hand, one can measure the the radial velocities of the members of the cluster—as had been done since the 1930's starting with the research of Zwicky (1933) on the Coma Cluster—and estimate the mass of the cluster using the virial theorem. These studies led to some of the earlier evidence for dark matter before it became a widely accepted hypothesis. By the end of 1970's, however, the first gravitational lens had been discovered by Walsh, Carswell, and Weymann (1979), and it offered a viable alternative for estimating the mass of the clusters responsible for the lensing, since the lensing effect is sensitive to the shape of the mass distribution of the gravitating body that creates it. A detailed discussion of mass determination from gravitational lensing is given by Hoekstra et al. (2013). Towards the end of the 1980's various instances of gravitational lenses

had been observed in distant clusters (Lynds and Petrosian 1989; Soucail et al. 1988), and the growing array of lensing data allowed for more detailed study of the mass distributions (Tyson, Valdes, and Wenk 1990).

Another line of observations to constrain the amount of dark matter in the universe, starting in the 1980's, came from measurements of the anisotropies in the cosmic microwave background (CMB) radiation. The CMB is formed out of the radiation that was released by the time of the matter–radiation decoupling, and its temperature anisotropies related to the density fluctuations in the primordial plasma, the dynamics of which are sensitive to the matter and energy content of the universe. In particular, the dark matter in the early universe is differentiated from regular baryonic matter by its property of being only gravitationally coupled to the rest of the plasma, and thus affecting the evolution of the density perturbation differently than baryonic matter. Starting with the launch of the RELIKT-1 and COBE satellites, the CMB anisotropy has been measured with ever increasing accuracy leading to the latest data from the Planck Collaboration (2018), which constrains the abundance of dark matter in the universe with supreme accuracy.

Although the CMB is the most abundant source of precision cosmological data, various other means of finding cosmological constraints have emerged. The Sloan Digital Sky Survey, starting in 2000 has produced an ever more precise picture of the distribution of luminous red galaxies through the Baryon Oscillation Spectroscopic Survey (BOSS), giving data about the present day large scale distribution of matter in the universe by means of redshift measurements. Just as the CMB anisotropy is a record of the early density perturbations, the distribution of galaxies gives the evolution of density perturbations to more recent times. The BOSS results have in particular been used to study the scale of the baryon acoustic oscillations imprinted on the matter distribution independently of the CMB (Ata et al. 2018), which offers another constraint on the present day abundance of dark matter. In the same vein of spectral measurements, observations of the spectra of light coming from distant quasars reveals the Lyman-α forest of absorption lines, which are the result of hydrogen gas clouds at different redshifts absorbing the light from the galaxies via the Lyman-α transition. The structure of the Lyman-α forest is sensitive to the cosmological model, and can thus be used to constrain cosmological parameters (Hernquist et al. 1996).

Perhaps the most compelling evidence in recent times for the dark matter hypothesis over the MOND theory comes from a study of the galaxy cluster known as the Bullet Cluster. Discovered in 1995 by Tucker, Tananbaum, and Remillard, the Bullet Cluster is a collision of two galaxy clusters. The bulk of its baryonic mass lies in a hot cloud of plasma that has been slowed down relative to the colliding clusters of galaxies, but observations of gravitational lensing show that the lensing is strongest at the location of the galaxy subclusters (Markevitch et al. 2004), suggesting under a standard interpretation that most of the gravitating mass is located within the galaxy subclusters that have passed through each other, rather than in the gas cloud where bulk of the baryonic mass is located. Clowe et al. (2006) have argued that this observation

is inconsistent with MOND, since the peak lensing in that theory still aligns with the peak mass density.

Although dark matter seems by far the most compelling explanation for a variety of phenomena in astrophysics and cosmology, it is not without its problems. In the early 1990's, Kauffmann, White, and Guiderdoni (1993) managed to demonstrate a semi-analytical model of galaxy formation including CDM halos that correctly reproduced a range of observations, but which also predicted a Milky Way sized galaxy should have a large number of, over a hundred, smaller satellite galaxies in its neighborhood. Further numerical simulations confirmed these results suggesting up to 500 satellites in the Local Group (Moore et al. 1999; Klypin et al. 1999). On the other hand, in the 1990's, only around ten satellites of Milky Way were known, and to this day the number of known satellites is around 50 (DES Collaboration 2015). More recent simulations show a similar trend as those from the 1990's (Springel et al. 2008). This discrepancy is known as the missing satellites problem. Various fixes have been suggested. At the simplest, it is plausible that no new physics is needed to explain the missing satellites. The original simulations did not include baryonic physics, which are expected to result in a smaller number of massive satellites and suppress star formation, leaving many of the satellites too dark to obeserve (Brooks et al. 2013; Sawala et al. 2016). Thus inclusion of the effects of baryonic matter and star formation may be all that is needed to resolve the issue. Other proposed solutions modify the dark matter physics by making the dark matter warmer (Colín, Avila-Reese, and Valenzuela 2000; Macciò and Fontanot 2010) or by introducing interactions within the dark sector (Vogelsberger, Zavala, and Loeb 2012).

Since the early 1990's, it has also been known that the density profiles of collisionless CDM halos in numerical simulations do not produce the observed behavior towards the center of the halo. Namely, the rotation velocities of galaxies towards the center are known to increase linearly with the radius, which is consistent with a near constant density around the center (Athanassoula, Bosma, and Papaioannou 1987; Begeman, Broeils, and Sanders 1991). On the other hand, simulations found density profiles much more steeply peaked at the center, following a distribution more resembling $\rho \sim r^{-1}$ (Dubinski and Carlberg 1991; Navarro, Eke, and Frenk 1996; Navarro, Frenk, and White 1997). This discrepancy between observations and simulations continues to this day. Suggested solutions to this problem again range from baryonic effects (Governato et al. 2012; Pontzen and Governato 2012), to interactions within the dark sector (Spergel and Steinhardt 2000; Loeb and Weiner 2011; Elbert et al. 2015), and warm dark matter (Colín, Avila-Reese, and Valenzuela 2000).

Despite these issues particular to the collisionless cold dark matter hypothesis, the existence of dark matter remains a very compelling hypothesis that manages to explain a wide variety of phenomena both in the realm of cosmology, as well as in the realm of astrophysics. In spite of the ability of the dark matter hypothesis to explain all these phenomena, however, its constitution still remains completely in the dark.

3.1 Dark matter models

The various candidates for dark matter are usually divided into two categories: baryonic dark matter, and nonbaryonic dark matter. Baryonic dark matter describes candidates that do not require any new exotic particles, but are simply made of known particles. Nonbaryonic dark matter, on the other hand, covers all the various possible extensions of the standard model that are suitable dark matter candidates.

Baryonic dark matter is most commonly discussed in the context of massive compact halo objects (MACHOs). MACHOs are objects composed of baryonic matter that for one reason or another emit too little electromagnetic radiation to be detectable from their luminosity. These include star-like objects—such as brown dwarves which never gained enough mass to sustain nuclear fusion, or white dwarves and neutron stars that are long lived enough to have cooled significantly—as well as rogue planets, and although not strictly speaking baryonic, also black holes. Although the existence of these kinds of objects is not controversial, and they likely contribute some portion of the dark mass of galaxies, observations suggest that MACHOs can only account for a small portion of the dark matter that is thought to exist (MACHO Collaboration 2000).

Since baryonic dark matter is an unlikely candidate to explain all the dark matter in the universe, the most widely believed hypothesis is that dark matter is a new particle or group of particles that does not exist in the standard model, and is very weakly coupled to the standard model particles. Despite the fact that quantum field theory in principle forms a restrictive framework on the types of interactions and particle species that can exist, the landscape of possible extensions to the standard model is nonetheless quite vast, and many of these extensions can accommodate some dark matter candidate if the couplings to standard model particles are small enough.

The earliest popular models for nonbaryonic dark matter were the so called weakly interacting massive particles (WIMPs), motivated by supersymmetric extensions of the standard model. Unifying theories remain the most prolific source of potential dark matter candidates since they offer not just an ad hoc candidate, but also an immediate explanation of how it fits the wider framework of physics. Discovery of a dark matter matter candidate with properties consistent with these theories would also lend them more credibility and give guidance in the unification of the fundamental forces. Examples of such models include mirror dark matter, which postulates a dark sector exactly equivalent to the standard model, motivated by $E_8 \times E_8$ superstring theories (Kolb, Seckel, and Turner 1985). Likewise, the kinetic mixing that is the topic of this thesis arises in any theory with a $U(1) \times U(1)$ symmetry, which turns out to be a property of various beyond standard model theories such as the aforementioned mirror symmetry with its two copies of $SU(3) \times SU(2) \times U(1)$, as well as in low-energy regimes of grand unified theories involving the breaking of $SO(10)$ and E_6 gauge groups, and of superstring theories where gauge groups break to these groups (Hewett and Rizzo 1989).

3.2 Direct detection searches

If dark matter exists and interacts weakly with visible matter, events produced by such interactions should be observable. There are a variety of dark matter dedicated for finding such a signature. Most of these experiments are based on searching for scatterings of dark matter particles off nuclei. Such detectors naturally observe large backgrounds from known scattering events, which need to be subtracted to reveal the dark matter signal. The lack of a signal places generic constraints on the DM–nucleus scattering cross section, which can be applied to any chosen dark matter model. The relevant scattering cross section can then be calculated in a given model to obtain bounds on the coupling and masses for that specific model.

Over the past decade, reports of signals from the CoGeNT and DAMA experiments have been made regarding an annual variation in the number of recorded events (Aalseth et al. 2014; Bernabei et al. 2018). Such a variation is expected in typical dark matter models, resulting from the variation of Earth's velocity with respect to the galactic dark matter halo as the Earth orbits the Sun. Likewise, the CDMS and CRESST-II experiments have also reported signals over the background (Angloher, Bauer, et al. 2012; CDMS Collaboration 2013) but the signal has not been seen in further runs of CRESST-II (Angloher, Bento, et al. 2014). Data from various other nuclear scattering experiments is in conflict with these signals (see results from the DarkSide Collaboration (2018) and the references within). Though the source of the annual modulation in the CoGeNT and DAMA data remains undetermined, other searches have managed to strongly constrain the DM–nucleus cross section at varying dark matter masses and to make the dark matter interpretation of the modulation suspect.

3.3 Generation of dark matter

Given a dark matter model, the most pressing question question that arises is how the present day dark matter density arises, and whether (or under what parameters) the model can produce the present day density. For particle theories of dark matter, this question is in principle straightforwardly answered in a unified framework of thermodynamics in the early universe, where the thermal distribution of every particle species evolves according to the Boltzmann equation derived in section 2.2. In practice, of course, the nonlinearity of the Boltzmann equations and the complexity of the interactions means that one often has to consider the picture with various simplifying approximations.

How strongly the dark matter interacts with the rest of the matter in the universe broadly speaking determines how it is generated. From the Boltzmann equation (2.10), it is readily apparent that the dark matter creation and annihilation processes which come in to the Boltzmann equation through the collision term on the right hand side compete with the expansion of the universe which affects the dark matter density through the Hubble rate H, and strictly

works to decrease it. If the rate of interactions is sufficiently great compared to the Hubble rate, the dark matter will be driven towards thermal equilibrium with the rest of the matter. However, with the expansion and cooling of the universe the rate of equilibrating processes will decrease until it inevitably falls below the Hubble rate at which point the dark matter essentially decouples from other matter and falls out of equilibrium and will from then on track the expansion rate of the universe ($n \propto a^{-3}$)—unless there are internal processes within the dark sector—leading to the present day density. This process of dark matter creation where the density is in equilibrium with the rest of the matter early on, and then falls out of equilibrium is generally known as the freeze out scenario, owing to the fact that the comoving number density $a^3 n$ freezes to its present day value once the rate of processes falls below the Hubble rate.

The freeze out scenario is a much studied one since it is the process by which WIMPs produce the present day relic abundance, and also because the initial equilibrium assumption justifies the use of equation (2.18). The popularity of WIMP dark matter originated in the observation that the present day relic density was consistent with that predicted by the freeze out scenario for a particle with mass and coupling in the electroweak range ($m \sim 100$ GeV, $g \sim 10^{-2}$), and such a particle was also well motivated by supersymmetry (Jungman, Kamionkowski, and Griest 1996). While the outlook for supersymmetry has become less probable since then, WIMPs remain a viable dark matter candidate.

It is, however, possible that the coupling of the dark matter to standard model particles might be far smaller than would be expected from a typical WIMP. In such a scenario it can happen that its interactions with the standard model particles are so weak that the interaction rate never manages to reach equilibrium with the visible sector. In this case, if the particle starts with a negligible abundance, its density will be too small to produce any significant annihilation or scattering to the visible sector, and the dark sector will slowly be filled by annihilations and scatterings from the visible sector, leading to the increase of the comoving number density with time until the present day value is reached. This process of dark matter creation is in contrast to freeze out known as the freeze in scenario, and the particles whose abundance is generated in this way are known as FIMPs in contrast to WIMPs, being feebly interacting instead of weakly interacting (or alternatively freezing in rather than of freezing out). The freeze in is essentially the other end of the spectrum from freeze out, and is useful because due to the negligible initial abundance the term for the reverse of the generating process in the collision term can be neglected. For some reviews of FIMP dark matter models, see for instance (Hall et al. 2010) and (Bernal et al. 2017).

The relatively large couplings of WIMPs means that they are tractable to direct detection either in collider experiments, or various other experiments dedicated to searching dark matter particles such as nucleon scattering. The lack of a WIMP signaling with ever increasing precision of experiments decreases the likelihood of WIMP dark matter. FIMPs skirt around this

issue by having couplings far too weak to produce significant signals in these experiments, since the coupling strength needed for the reaction rate to remain below the Hubble rate is often well below what can be detected directly. The hope is of course that next generation searches would eventually be able to probe the FIMP regime and put constraints on the parameter space.

Apart from the freeze in and freeze out scenarios, the dark matter generation may be more complex if the dark sector itself contains interactions, as is the case with many more complicated models. If the dark sector has internal dynamics, the dark matter density may evolve in nontrivial ways even when the dark sector is decoupled from the visible sector. In particular, in the freeze in scenario the dark matter can generally be nonthermal if there are no interactions that would allow the dark sector particles to distribute their energy to reach an equilibrium distribution, and thus have a well defined temperature. If, however, there exists some interaction in the dark sector that enables dark matter scattering, but the coupling of the dark sector to the visible sector remains small, the dark sector can reach an internal thermal equilibrium characterized by some temperature that is different from the temperature of the visible plasma. The interactions in the dark sector may eventually decouple just as the dark sector decouples from the visible sector in the freeze out scenario. This scenario is known as a dark freeze out due to its similarities with the standard freeze out scenario.

Depending on the exact contents of the dark sector, the dynamics can get very complicated. If the dark sector contains various interacting particle species, then entropy may flow between the different species, the different interactions may decouple at different times, and massive particles will become nonrelativistic at different times. We will not be discussing more complex dynamics beyond the assumption that the dark sector can be in thermal equilibrium by itself without being in thermal equilibrium with the visible sector.

4 DARK SECTOR WITH KINETIC MIXING

The main subject of this thesis is a dark sector addition to the Standard model Lagrangian consisting of an additional U(1) gauge field, and extended to possibly contain other particles, mainly fermions, that do not have any other couplings to the standard model. Models with two U(1) fields have been studied in theoretical physics literature since the 1980's (Okun 1982; Galison and Manohar 1984; Holdom 1986) with Goldberg and Hall (1986) even discussing them in the context of dark matter. However, only in the recent years have such models become popular as dark matter candidates. The peculiarity of having an U(1) × U(1) symmetry in the Lagrangian is that, since the group is Abelian, the field strength associated to it is gauge invariant. Hence if the standard quantum field theory prescription of including all renormalizable Lorentz and gauge invariant terms in the Lagrangian is followed, the Lagrangian includes a kinetic mixing term involving the field strengths of the two U(1) fields. Concretely, we will consider a Lagrangian of the form

$$\mathcal{L} = \mathcal{L}_{\mathrm{SM}} + \mathcal{L}_{\mathrm{D}},$$

where $\mathcal{L}_{\mathrm{SM}}$ contains all the standard model terms and

$$\mathcal{L}_{\mathrm{D}} = -\frac{1}{4}\hat{X}_{\mu\nu}\hat{X}^{\mu\nu} - \frac{\sin\varepsilon}{2}B_{\mu\nu}\hat{X}^{\mu\nu} + \frac{1}{2}\hat{m}_X^2\hat{X}^{\mu}\hat{X}_{\mu} + \bar{\chi}i\not{D}\bar{\chi} + m_\chi\bar{\chi}\chi, \qquad (4.1)$$

where $\frac{1}{2}\sin\varepsilon B_{\mu\nu}\hat{X}^{\mu\nu}$ is the kinetic mixing term. Here B is the hypercharge U(1) field of the Standard Model, $\hat{X}$ is the new U(1) gauge field, and χ is a potential fermion that only couples to $\hat{X}$ through the covariant derivative $D_\mu = \partial_\mu + ig_X\hat{X}_\mu$. The parameter ε here is the kinetic mixing angle which determines how strongly the dark photon couples to the standard model. It will be useful sometimes to denote this model by SM + U(1) + χ, or just SM + U(1) if no dark fermion is involved.

It turns out that with a suitable change of basis, the kinetic terms can be transformed into their canonical (i.e., diagonal) form. This introduces ε-dependent couplings of Standard Model gauge fields to χ, and of X to Standard Model fermions, as well as some corrections to Standard Model parameters. These corrections will generally change some predictions of the Standard Model, which sets bounds on the size of ε and m_X directly from collider data. However, since we are regarding $\hat{X}$ and χ as dark particles, ε will be assumed to be very small. This means that the bounds coming from current collider experiments will not significantly limit the parameters in the relevant part of the parameter space, since the relevant effects of the

dark sector on experimental parameters will generally be suppressed by terms proportional to ε^2 and higher powers.

In the following sections, the distinction of whether $\hat{X}$ has a mass or not will turn out to be important. In particular, we will see that if $\hat{X}$ is massless SM + U(1) does not produce observable changes to the parameters of the model at any loop order, and that in SM + U(1) + χ the only corrections to Standard Model observables come from χ loops.

4.1 The massive case

We begin the analysis of the model by assuming that $\hat{m}_X \neq 0$. We will take the mass here as given, and not consider its origin. The main computations done here will then be mostly applicable in the limit $\hat{m}_X \to 0$ with few notable exceptions. We can write the kinetic and mass terms of the Lagrangian schematically as

$$-\frac{1}{4}\hat{F}^{\mathsf{T}}_{\mu\nu} K \hat{F}^{\mu\nu} + \frac{1}{2}\hat{F}^{\mathsf{T}}_{\mu} M^2 \hat{F}^{\mu}.$$

Here $\hat{F}$ denotes a vector with components $(\hat{X}, B, W_3)$, with W_3 being the third component of the SU(2) gauge field. The matrix K is a kinetic mixing matrix, given in this basis by

$$K = \begin{pmatrix} 1 & s_\varepsilon & 0 \\ s_\varepsilon & 1 & 0 \\ 0 & 0 & 1 \end{pmatrix},$$

where s_ε stands for $\sin\varepsilon$, and M^2 is a mass matrix, which in this basis is

$$M^2 = \hat{m}_Z^2 \begin{pmatrix} C^2 & 0 & 0 \\ 0 & \hat{s}_W^2 & -\hat{s}_W\hat{c}_W \\ 0 & -\hat{s}_W\hat{c}_W & \hat{c}_W^2 \end{pmatrix},$$

where $\hat{s}_W$ and $\hat{c}_W$ are the sine and cosine of the standard model Weinberg angle, defined by

$$\hat{c}_W = \frac{g}{\sqrt{g^2 + g'^2}}, \quad \text{and} \quad \hat{s}_W = \frac{g'}{\sqrt{g^2 + g'^2}},$$

with g and g' being the usual SU(2) and U(1) gauge couplings of the standard model. The parameter $C^2 = \hat{m}_X^2/\hat{m}_Z^2$, with $\hat{m}_Z$ being the usual Z-boson mass. For the standard photon and Z-boson defined by $\hat{A} = \hat{c}_W B + \hat{s}_W W_3$ and $\hat{Z} = -\hat{s}_W B + \hat{c}_W W_3$ this matrix gives the usual mass term $\frac{1}{2}\hat{m}_Z^2 \hat{Z}_\mu \hat{Z}^\mu$.

We want to find a basis where the Lagrangian is in its canonical form, i.e., where K takes the form of a unit matrix, and M^2 is diagonal. It is always possible to find such a basis since there always exists a nonsingular matrix P such that $\hat{F} = P\hat{F}'$ $P^{\mathsf{T}} K P = I$, after which the kinetic term obtains its canonical form $\hat{F}^{\mathsf{T}}\hat{F}$ which is invariant under all orthogonal basis transformations, and this freedom can then be used to diagonalize the mass

matrix. The relevant matrix P in this case is given by

$$P = \begin{pmatrix} c_\varepsilon^{-1} & 0 & 0 \\ -t_\varepsilon & 1 & 0 \\ 0 & 0 & 1 \end{pmatrix}.$$

After this we can write $\hat{F}' = O_W \hat{F}''$, where

$$O_W = \begin{pmatrix} 1 & 0 & 0 \\ 1 & \hat{c}_W & -\hat{s}_W \\ 0 & \hat{s}_W & \hat{c}_W \end{pmatrix}.$$

This transformation diagonalizes the lower 2×2 block of the mass matrix such that

$$M''^2 = \hat{m}_Z^2 \begin{pmatrix} c_\varepsilon^{-2} C^2 + t_\varepsilon^2 \hat{s}_W^2 & 0 & t_\varepsilon \hat{s}_W \\ 0 & 1 & 0 \\ t_\varepsilon \hat{s}_W & 0 & 1 \end{pmatrix}.$$

Next we define a second orthogonal matrix

$$O_\xi = \begin{pmatrix} c_\xi & 0 & -s_\xi \\ 0 & 0 & 0 \\ s_\xi & 0 & c_\xi \end{pmatrix}.$$

The angle ξ is defined by the condition that this matrix should diagonalize M''^2, which gives the condition

$$\frac{t_\xi}{1 - t_\xi^2} = -\frac{\hat{s}_W t_\varepsilon}{1 - \hat{s}_W^2 t_\varepsilon^2 - C^2/c_\varepsilon^2}. \tag{4.2}$$

In terms of the basis $F = (X, A, Z)$ in which the Lagrangian has its canonical form the original basis $\hat{F}$ is

$$\begin{pmatrix} \hat{X} \\ B \\ W_3 \end{pmatrix} = \begin{pmatrix} c_\varepsilon^{-1} & 0 & 0 \\ -t_\varepsilon & 1 & 0 \\ 0 & 0 & 1 \end{pmatrix} \begin{pmatrix} 1 & 0 & 0 \\ 0 & \hat{c}_W & -\hat{s}_W \\ 0 & \hat{s}_W & \hat{c}_W \end{pmatrix} \begin{pmatrix} c_\xi & 0 & -s_\xi \\ 0 & 1 & 0 \\ s_\xi & 0 & c_\xi \end{pmatrix} \begin{pmatrix} X \\ A \\ Z \end{pmatrix}. \tag{4.3}$$

This leads to the field redefinitions

$$\begin{aligned} \hat{X} &= c_\varepsilon^{-1} c_\xi X - c_\varepsilon^{-1} s_\xi Z \\ B &= -(\hat{s}_W s_\xi + t_\varepsilon c_\xi) X + \hat{c}_W A + (s_\xi t_\varepsilon - \hat{s}_W c_\xi) Z \\ W_3 &= \hat{c}_W s_\xi X + \hat{s}_W A + \hat{c}_W c_\xi Z. \end{aligned}$$

The couplings of the B and W_3 fields to fermions are given by $-\bar{f}[g' Q \not{B} + (g \not{W}_3 - g' \not{B}) T_3 P_L]$, where T_3 is the third component of weak isospin, and Q is the electric charge defined from the weak isospin and weak hypercharge Y as $Q = T_3 + \frac{1}{2} Y$. This gives the following standard model fermion couplings:

$$-\hat{e} Q \bar{f} \not{A} f, \tag{4.4}$$

$$\frac{\hat{e}}{\hat{c}_W \hat{s}_W} c_\xi \bar{f} \not{Z} [g_{fV}^Z - g_{fA}^Z \gamma^5] f, \tag{4.5}$$

$$\frac{\hat{e}}{\hat{c}_W \hat{s}_W} c_\xi \bar{f} \not{X} [g_{fV}^X - g_{fA}^X \gamma^5] f, \tag{4.6}$$

where

$$g_{fA}^{Z} = \tfrac{1}{2}T_3(1 - \hat{s}_W t_\varepsilon t_\xi), \qquad g_{fV}^{Z} = Q(\hat{s}_W^2 - \hat{s}_W t_\varepsilon t_\xi) + g_{fA}^{Z}, \tag{4.7}$$

$$g_{fA}^{X} = \tfrac{1}{2}T_3(\hat{s}_W t_\varepsilon + t_\xi), \qquad g_{fV}^{Z} = Q(\hat{s}_W t_\varepsilon + \hat{s}_W^2 t_\xi) + g_{fA}^{X}. \tag{4.8}$$

It is useful to note that in the limit of small ε these are given by

$$g_{fA}^{Z} = \tfrac{1}{2}T_3 + \mathcal{O}(\varepsilon^2), \qquad g_{fV}^{Z} = Q\hat{s}_W^2 + g_{fA}^{Z} + \mathcal{O}(\varepsilon^2), \tag{4.9}$$

$$g_{fA}^{X} = \mathcal{O}(\varepsilon^2), \qquad g_{fV}^{Z} = Q\hat{s}_W\hat{c}_W^2\varepsilon + \mathcal{O}(\varepsilon^2). \tag{4.10}$$

The couplings to χ are

$$-g_X c_\varepsilon^{-1} c_\xi \bar{\chi} \not{X} \chi, \quad -g_X c_\varepsilon^{-1} s_\xi \bar{\chi} \not{Z} \chi. \tag{4.11}$$

Notable here is that the coupling of the massless field A which we naturally associate with the electromagnetic field remains unchanged. This suggests that we can simply define $e \equiv \hat{e}$ to be the physical electromagnetic coupling. We will see that this is the case when we define the input parameters of the model in terms of physical observables.

The main noteworthy feature here is that the mixing generates a coupling of the field X to Standard Model fermions. This creates a production and decay channel for X. If the dark fermion χ is included in the model with a non-negligible coupling to $\hat{X}$, then the X particles produced quickly decay to χ. However, if there are no new fermions, X can only decay to Standard Model fermions. If the mixing parameter ε is very small, and $\hat{m}_X$ is not too close to $\hat{m}_X$, then the coupling for $\bar{f}\not{X}f$ is of the order ε, which allows for possibly very long lived X particles that might serve as a dark matter candidate. This possibility has been studied by Redondo and Postma (2009) as well as by Fradette et al. (2014).

From the diagonalized matrix we obtain the X and Z masses

$$m_X^2 = \hat{m}_Z^2(1 + \hat{s}_W t_\varepsilon t_\xi^{-1}), \quad \text{and} \quad m_Z^2 = \hat{m}_Z^2(1 - \hat{s}_W t_\varepsilon t_\xi).$$

If we want to express the X mass in terms of the mass parameter $\hat{m}_X$ rather than in terms of $\hat{m}_Z$, we can use the relation

$$\frac{\hat{m}_X^2}{\hat{m}_Z^2} = (1 + \hat{s}_W t_\varepsilon t_\xi^{-1})(1 - \hat{s}_W t_\varepsilon t_\xi)c_\varepsilon^2$$

obtained from the condition (4.2). This lets us write

$$m_X^2 = \frac{\hat{m}_X^2}{c_\varepsilon^2(1 - \hat{s}_W t_\varepsilon t_\xi)}, \quad \text{and} \quad m_Z^2 = \hat{m}_Z^2(1 - \hat{s}_W t_\varepsilon t_\xi).$$

4.1.1 Physical parameters and observables

In order to make contact with experiment, it is useful to write the model in terms of parameters that can be easily measured in experiments. These input

parameters in standard electroweak theory are the fine structure constant α, the Fermi coupling G_F, and the Z-boson mass m_Z.

In practice, the fine structure constant is determined from low-energy scattering of fermions, which in the language of QFT is governed by the amplitude given at tree level by the diagram

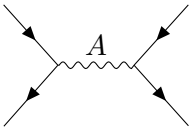

This gives the fine structure constant $\alpha \equiv \hat{e}^2/4\pi$, which justifies the definition of the physical electric charge $e \equiv \hat{e}$.

The Fermi coupling is obtained from the muon lifetime, and is determined by the process $\mu^- \to \nu_\mu \bar{\nu}_e e^-$. At tree level this process is mediated by the the W-boson, leading to the definition of the Fermi coupling

$$G_F \equiv \frac{\sqrt{2}}{8}\frac{g^2}{\hat{m}_W^2} = \frac{\sqrt{2}}{8}\frac{\hat{e}^2}{\hat{m}_W^2 \hat{s}_W^2}.$$

Notice that the charged interactions are completely unaffected by the introduction of the field $\hat{X}$, and thus, like the electromagnetic coupling, the Fermi coupling receives no corrections to its Standard Model value. Since we have the equality $e \equiv \hat{e}$ between the physical electric charge and the theoretical parameter, and $\hat{m}_W = m_W$ is the physical mass of the W-boson because the charged part of the weak sector is unaffected, the right hand side suggests the definition of a physical weak mixing angle $s_F \equiv \sin\theta_F \equiv \hat{s}_W$.

The mass of the Z-boson is defined by the pole of its propagator. Apart from loop corrections, again, this definition gives the physical mass $m_Z^2 = \hat{m}_Z^2(1 - \hat{s}_W t_\varepsilon t_\xi)$.

In standard electroweak theory, there is a relation $m_W^2 = m_Z^2 c_W^2$ between the weak boson masses and the weak mixing angle. In the SM + U(1) model this relation holds for the hatted parameters, $\hat{m}_W^2 = \hat{m}_Z^2 \hat{c}_W^2$. However, with the above definitions of the physical parameters, it is clear that the relation between m_W, m_Z, and c_F is nontrivial, since the Z mass is modified. However, alternatively it is possible to define the weak mixing angle by $c_M^2 \equiv \cos^2\theta_M \equiv m_W^2/m_Z^2$. The previous definition based on the Fermi parameter is preferred, however, since it gives a nontrivial value for the ρ-parameter

$$\rho \equiv \frac{m_W^2}{m_Z^2 c_W^2},$$

where c_W is now the cosine of whatever we define as our physical weak mixing angle. Then $\rho - 1$ is zero in the Standard Model, but nonzero otherwise. From the definitions given above that the tree level expression for ρ in this model is

$$\rho = \frac{1}{1 - s_F t_\varepsilon t_\xi} \approx 1 + s_F t_\varepsilon t_\xi,$$

where the last approximation holds under the assumption that ε is small and t_ξ is not too large.

Another interesting observable is the muon magnetic moment, which has a significant discrepancy between the experimental value and the computed standard model value. Namely, the difference between the experimental and standard model values is $\delta a_\mu = a_\mu^{\text{exp}} - a_\mu^{\text{SM}} = 268 \times 10^{-11}$, which is a 3.5σ difference according to latest data from the Particle Data Group (2018). The massive dark photon contributes to the anomalous magnetic moment in two ways. On one hand, it modifies the Z-boson coupling in an observable way, as seen from the analysis of the ρ-parameter. In addition, the dark photon gives a new loop contribution to the magnetic moment via the diagram

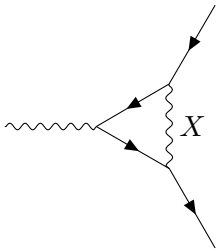

In general, a standard computation of the above loop for an arbitrary fermion f coupling to a massive vector boson U via $-g\bar{f}\not{U}(g_{fV}^U + g_{fA}^U\gamma^5)f$ is given by

$$g^2\frac{(g_{fV}^U)^2K(m_f^2/m_U^2) - 5(g_{fA}^U)^2H(m_f^2/m_U^2)}{12\pi^2}\frac{m_f^2}{m_U^2},$$

where

$$K(Y) = 3\int_0^1 \frac{x^2(1-x)}{x^2Y + 1 - x}\,dx, \quad H(Y) = \frac{3}{5}\int_0^1 \frac{2x^3Y + x(1-x)(4-x)}{x^2Y + (1-x)}\,dx.$$

In the case $Y \ll 1$ we have $K(Y) \approx H(Y) \approx 1$, and when $Y \gg 1$ we have $H(Y) \approx 3/5$ and $K(Y) \approx 3/2Y$.

The contribution from X to the anomalous magnetic moment is now straightforward to see. Extracting the contribution of the modified Z-boson couplings is less straightforward since rather than being a linear contribution to a_μ, it is a modification on the Z contribution. In the limit of small mixing, one can take the lowest order change, in which case we may write

$$\delta a_\mu = \frac{e^2}{s_F^2c_F^2}\left(\frac{(g_{\mu V}^X)^2K_{\mu X} - 5(g_{\mu A}^X)^2H_{\mu X}}{12\pi^2}\frac{m_f^2}{m_X^2} + \Delta_\varepsilon\frac{(g_{\mu V,0}^Z)^2K_{\mu Z} - 5(g_{\mu A,0}^Z)^2H_{\mu Z}}{12\pi^2}\frac{m_f^2}{m_Z^2}\right) \tag{4.12}$$

Here Δ_ε is a ε dependent contribution, and $g_{\mu V,0}^Z$ and $g_{\mu A,0}^Z$ are the $\varepsilon = 0$ forms of these couplings. There is a further complication here regarding the limit of small m_X. In this limit H becomes constant, so the axial term appears singular at $m_X = 0$. According to Fayet (2007) this singularity is only apparent since

the ratio of the couplings to m_X is fixed by the U(1) symmetry breaking scale. However, a detailed discussion is beyond the scope of this thesis.

Apart from the muon anomalous magnetic moment, the theory is of course naturally also constrained by the electron magnetic moment and its lack of significant discrepancy from the standard model predicted value. Deviations from the standard model value relative to the muon, however, are suppressed by the much smaller mass of the electron, so even though the electron anomalous magnetic moment is more constrained, the constraints on the mixing are not necessarily better.

4.2 The massless case

In the previous section we saw how the addition of a massive U(1) field with kinetic mixing modifies the Standard Model interactions and observables. In this section we will consider the special case where $\hat{m}_X$ is set to zero. Doing this has two main effects. First, the eigenvalues of the mass matrix M''^2 in equation (4.1) become degenerate, and after diagonalization it has the form

$$\hat{m}_Z^2 \begin{pmatrix} 0 & 0 & 0 \\ 0 & 0 & 0 \\ 0 & 0 & 1+\hat{s}_W^2 t_\varepsilon^2 \end{pmatrix}.$$

Crucially, the degeneracy of the mass matrix implies that having canonical kinetic and mass terms does not uniquely determine the basis. Rather, the diagonalized mass matrix is invariant under arbitrary O(2) transformations of the form

$$\pm \begin{pmatrix} c_\beta & -s_\beta & 0 \\ s_\beta & c_\beta & 0 \\ 0 & 0 & 1 \end{pmatrix}.$$

Which component of O(2) the matrix is in does not make a significant difference for the following discussion, so for sake of convenience we will assume that the above matrix comes with a plus sign. Then the most general transformation that takes the Lagrangian to its canonical form is given by

$$\begin{pmatrix} \hat{X} \\ B \\ W_3 \end{pmatrix} = \begin{pmatrix} c_\varepsilon^{-1} & 0 & 0 \\ -t_\varepsilon & 1 & 0 \\ 0 & 0 & 1 \end{pmatrix} \begin{pmatrix} 1 & 0 & 0 \\ 0 & \hat{c}_W & -\hat{s}_W \\ 0 & \hat{s}_W & \hat{c}_W \end{pmatrix} \begin{pmatrix} c_\xi & 0 & -s_\xi \\ 0 & 1 & 0 \\ s_\xi & 0 & c_\xi \end{pmatrix} \begin{pmatrix} c_\beta & -s_\beta & 0 \\ s_\beta & c_\beta & 0 \\ 0 & 0 & 1 \end{pmatrix} \begin{pmatrix} X \\ A \\ Z \end{pmatrix},$$

with β arbitrary.

The second main effect of removing the X mass is that the definition of t_ξ simplifies greatly. From (4.2) we see by putting $C^2 = 0$ that

$$t_\xi = -\hat{s}_W t_\varepsilon.$$

This relation allows the writing of the relevant couplings in a simpler form. Applying this, we get that the old fields in terms of the new ones are

$$\hat{X} = c_\varepsilon^{-1} c_\xi c_\beta X - c_\varepsilon^{-1} c_\xi s_\beta A - c_\varepsilon^{-1} s_\xi Z, \tag{4.13}$$

$$B = \hat{c}_W(s_\beta - c_\beta c_\xi \hat{c}_W t_\varepsilon)X + \hat{c}_W(c_\beta + s_\beta c_\xi \hat{c}_W t_\varepsilon)A - \hat{s}_W c_\xi (1+t_\varepsilon^2)Z, \tag{4.14}$$

$$W_3 = (\hat{s}_W s_\beta + \hat{c}_W s_\xi c_\beta)X + (\hat{s}_W c_\beta - \hat{c}_W s_\xi s_\beta)A + \hat{c}_W c_\xi Z. \tag{4.15}$$

These field redefinitions lead to the couplings

$$-\hat{e}(c_\beta + s_\beta \hat{c}_W c_\xi t_\varepsilon) Q \bar{f} \not{A} f, \quad -\hat{e}(s_\beta - c_\beta \hat{c}_W c_\xi t_\varepsilon) Q \bar{f} \not{X} f, \tag{4.16}$$

and

$$-\frac{\hat{e}}{\hat{c}_W \hat{s}_W} c_\xi \bar{f} \not{Z} [-Q \hat{s}_W^2 (1 + t_\varepsilon^2) + T_3 (1 + \hat{s}_W^2 t_\varepsilon^2) P_L] f \tag{4.17}$$

for the standard model particles, and to the couplings

$$-g_X c_\varepsilon^{-1} c_\xi c_\beta \bar{\chi} \not{X} \chi, \quad g_X c_\varepsilon^{-1} c_\xi s_\beta \bar{\chi} \not{A} \chi, \quad -g_X c_\varepsilon^{-1} s_\xi \bar{\chi} \not{Z} \chi \tag{4.18}$$

to χ. The shift to the Z-boson mass is unaffected by the angle β since the transformation O_β leaves the mass terms invariant. Thus $m_Z^2 = \hat{m}_Z^2 (1 + \hat{s}_W^2 t_\varepsilon^2)$.

4.2.1 Physical parameters and observables

In the case where the field X is massive, the determination of what was physical in the theory was in some sense straightforward because the condition that the Lagrangian has its canonical form (i.e., diagonal kinetic and mass terms) uniquely determines basis. However, when the mass is taken to zero, the same condition only determines the basis up to an arbitrary O(2) transformation, parametrized here by the angle β. The principle of basis invariance would suggest that the choice of β is irrelevant, and any choice should lead to the same physics. However, on the basis of the interaction terms (4.16) and (4.18) it is highly nontrivial whether this should actually be so, since the couplings of A and X to fermions are functions of β.

In this subsection we will carefully determine the parameters of the theory that can be directly determined from experiment as we did in subsection 4.1.1 for the massive case. In course of this we will see that, being diligent enough with what is observable in the theory, the dependence on β should vanish from all physical observables.

As in subsection 4.1.1, we have the standard input parameters α, G_F, and m_Z, which are defined by low-energy electron scattering, muon decay, and the Z-propagator pole, respectively. The Fermi coupling G_F and the Z-boson mass are given at tree level as one would expect by

$$G_F = \frac{\sqrt{2}}{8} \frac{\hat{e}^2}{\hat{m}_W^2 \hat{s}_W^2}, \quad \text{and} \quad m_Z^2 = \hat{m}_Z^2 (1 + \hat{s}_W^2 t_\varepsilon^2).$$

Note that in m_Z we have used the relation $t_\xi = -\hat{s}_W t_\varepsilon$ to simplify the expression, which only applies in the massless limit. In terms of t_ξ the expression is identical to the massive case.

When it comes to the definition of α, however, care has to be taken. Naively, one would expect on the basis of (4.16) that $\hat{e}(c_\beta + s_\beta \hat{c}_W c_\xi t_\varepsilon) = \sqrt{4\pi\alpha}$, which would be equivalent to determining α from the diagram

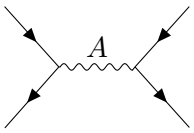

However, since X also couples to fermions and behaves in every way identically to A apart from the strength of its couplings to fermions, one also has to take into account the diagram

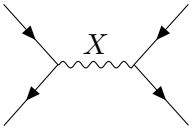

Since these diagrams have the same kinematic dependence, they both contribute to the electric charge. The physical fine structure constant is a multiplicative coefficient of the amplitude which at tree level is given by the sum of these two diagrams. Thus it is given by

$$4\pi\alpha = \hat{e}^2(c_\beta + s_\beta \hat{c}_W c_\xi t_\varepsilon)^2 + \hat{e}^2(s_\beta - c_\beta \hat{c}_W c_\xi t_\varepsilon)^2 = \hat{e}^2(1 + \hat{c}_W^2 c_\xi^2 t_\varepsilon^2). \quad (4.19)$$

Based on this definition of the fine structure constant, we define the physical electric charge by $e^2 \equiv \hat{e}^2(1 + \hat{c}_W^2 c_\xi^2 t_\varepsilon^2)$.

We can then define a physical weak mixing angle via the Fermi coupling by

$$G_F = \frac{\sqrt{2}}{8}\frac{e^2}{m_W^2 s_F^2},$$

where it follows that $s_F^2 = \hat{s}_W^2(1 + \hat{c}_W^2 c_\xi^2 t_\varepsilon^2)$. Using $c_\xi^{-2} = 1 + t_\xi^2$, we can write

$$s_F^2 = \hat{s}_W^2 \frac{1 + t_\varepsilon^2}{1 + \hat{s}_W^2 t_\varepsilon^2}.$$

Defining $c_F^2 = 1 - s_F^2$ gives

$$c_F^2 = \hat{c}_W^2 \frac{1}{1 + \hat{s}_W^2 t_\varepsilon^2}.$$

Notice that this immediately leads to the relation

$$\frac{m_W^2}{m_Z^2 c_F^2} = \frac{\hat{m}_W^2}{\hat{m}_Z^2 \hat{c}_W^2} = 1.$$

Therefore in the massless case the ρ parameter remains unmodified at tree level. More generally, we can write Z-boson interaction with standard model fermions from (4.17) in terms of these physical parameters we have defined, which leads to the expression

$$-\frac{e}{2c_F s_F}\bar{f}\not{Z}[(T_3 - 2Qs_F^2) - T_3\gamma^5]f.$$

This is identical to the usual standard model expression.

It can be shown that all amplitudes that contain no external A or X states are independent of β. The main principle is the observation that for any internal A propagator there exists a corresponding Feynman diagram for the process where the A propagator has been replaced with an X propagator.

These diagrams can then be combined to one diagram with a massless gauge propagator where the effective coupling on both vertices between fermions is

$$\begin{aligned} f &\leftrightsquigarrow f : \hat{e}\sqrt{(1+\hat{c}_W^2 c_\xi^2 t_\varepsilon^2)}, \\ \chi &\leftrightsquigarrow \chi : g_X c_\varepsilon^{-1} c_\xi, \\ f &\leftrightsquigarrow \chi : \sqrt{\hat{e} g_X s_\varepsilon} c_\xi c_\varepsilon^{-1}. \end{aligned}$$

The same also happens with all combinations of fermion, gauge triple and quadratic, and Higgs vertices, not shown here. Then the combinatorics always works out such that sums over diagrams with A and X vertices reduce to sums over diagrams with these effective vertices. It immediately follows from this that the anomalous magnetic moment a_f of a fermion can only be modified from its standard model value by loops involving χ. Indeed, if one takes care in computing the one loop value of a_e, the contribution from the diagrams

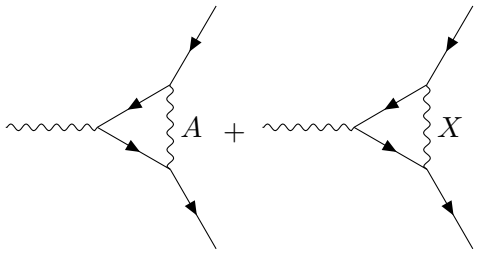

sums to give $a_e = \alpha/2\pi$, where α is precisely the physical fine structure constant given by (4.19).

When it comes to processes with external A and X states, these can generally have amplitudes involving β dependence. For instance, the Higgs decay rate $\Gamma(h \to AX)$ that occurs through a fermion loop is found to be proportional to $c_\beta s_\beta(1 - \hat{c}_W^2 c_\xi^2 t_\varepsilon^2) + (s_\beta^2 - c_\beta^2)\hat{c}_W c_\xi t_\varepsilon$. It then follows that the ratio

$$\frac{\mathrm{Br}(h \to AX)}{\mathrm{Br}(h \to AA)}$$

depends on the value of β. However, this ratio is not physically meaningful since the branching ratios $\mathrm{Br}(h \to AX)$ and $\mathrm{Br}(h \to AA)$ are not truly observable. This is because any A detection event is indistinguishable from a detection of X. Thus any detector will not be able to distinguish between decays $h \to AX$ and $h \to AA$. Alternatively, the amplitude being measured by a particle detector is not the amplitude for the process, but the amplitude for the process and a detection. That is, in practice, since any detector is made of fermions, all measuring processes only ever involve external fermion states, and as shown above, the amplitudes for such processes are independent of β.

The ramification of the above argument is that the theory SM + U(1) without any symmetry breaking in the extra U(1) sector gives the same predictions for all particle physics experiments as plain SM. This is traceable to the fact that the extra U(1) field can always be "rotated out" from the interaction terms of the Lagrangian if it does not initially have any couplings

to SM fermions, leaving a free background gauge field. If the fermion χ that couples to X is included, then it always interacts with SM fermions and produces measurable effects. Alternatively, as seen in the previous section, breaking of the extra U(1) symmetry uniquely determines the basis for the canonical Lagrangian, thus also producing measurable effects. In light of this, when discussing SM + U(1) + χ as a dark matter candidate, we will choose the convenient basis where only one massless boson interacts with the SM fermions, and this will by definition be identified as the usual photon.

4.3 Dark matter via kinetic mixing

In the previous sections we saw how the kinetic mixing leads to on one hand couplings of the dark photon to standard model fermions, and on the other hand of dark fermions to the standard model fields (namely Z when O(2) invariance was used to rotate out the interactions of the dark photon with standard model fermions) when the Lagrangian was brought to a canonical form. For small ε the strengths of these couplings turn out to be proportional to the weak mixing angle ε. There were four distinct possibilities with different behavior determined by whether or not the dark sector contains fermions, and whether or not the dark photon field X has a mass. The case where both are in the negative; that is, there are no dark fermion, and the dark photon is massless led to a curious situation where the field could be rotated to have no dynamics. This can obviously be ruled out as a dark matter candidate since it has two fatal flaws, namely that there is no way to generate the dark matter abundance since the dark matter is by definition noninteracting, and it is massless so it cannot be gravitationally bound.

However, in the case where the dark photon has a mass, we saw that the condition that the canonical basis is uniquely fixed, and so we have a well defined dark photon that couples to standard model fermions via couplings that are analogous to the Z-boson couplings and proportional to ε. Since the decay $X \to f\bar{f}$ given by the diagram

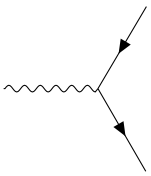

is allowed for massive vectors, the massive dark photon is unstable and in due time all of them will decay to standard model particles (provided its mass exceeds at least the lightest neutrino mass). However, the decay rate is suppressed by a factor of ε^2 from the interaction vertex, and is proportional to the mass of X. Namely, the decay rate using the vertex factor given by (4.6) is

$$\Gamma = \frac{1}{3}\frac{\alpha}{\hat{c}_W^2 \hat{s}_W^2} c_\xi^2 m_X \sqrt{1 - \frac{4m_f^2}{m_X^2}} \left((g_{fV}^X)^2 + (g_{fA}^X)^2 + 2((g_{fV}^X)^2 - 2(g_{fA}^X)^2)\frac{m_f^2}{m_X^2} \right),$$

where g_{fV}^X and g_{fA}^X are as given by (4.8), and α is the fine structure constant. For small mixing angles g_{fV} and g_{fA} are proportional to ε, and thus

$$\tau \sim \frac{1}{\varepsilon^2 m_X} \approx \frac{2 \times 10^{-29}}{\varepsilon^2} \times \frac{\text{MeV}}{m_X} \text{ y}.$$

The lifetime puts strong constraints on the size of ε, since it needs to be of the order of the age of the universe to not have all dark matter decay by present day. This means that we would need to require, for instance, $\varepsilon < 10^{-19}$ for a MeV scale dark photon. Note that the results here differ slightly from those of Fradette et al. (2014) since we mix the extra U(1) with the weak hypercharge field rather than with the electromagnetic field.

When fermions are added to the dark sector, the dark photon becomes a dynamic element of the dark sector that does not necessarily contribute significantly to the dark matter density. In this case the dark photon can be either massless or massive. In the case it is massless the O(2) invariance can be used to choose a convenient basis for how the two U(1) fields that remain after electroweak symmetry breaking couple to matter. There are two useful choices that can be made: such that only one field couples to the dark fermions, or such that only one couples to the standard model fermions. Although the massless variables A and X in equations (4.13)–(4.15) have been named suggestively, it is entirely arbitrary which we consider as the visible photon and which as the dark photon. Rather, we choose the basis such that A is obviously the particle that should be identified with the photon. Thus the first of the two basis choices presented corresponds to to the choice $t_\beta = 0$ while the second corresponds to the choice $t_\beta = \hat{c}_W c_\xi t_\varepsilon$. We will use the second choice in this thesis. Thus the U(1) couplings become

$$-e\bar{f}Q\not{A}f, \quad -g_X\bar{\chi}\not{X}\chi, \quad g_X c_W t_\varepsilon \bar{\chi}\not{A}\chi, \tag{4.20}$$

where e and c_W are physical quantities as discussed in section 4.2.1. In addition we have the Z-couplings from equations (4.17) and (4.18). It is again worth stressing that while there is an apparent modification to the electric charge and the Z-boson couplings to the standard model fermions, these modifications are absorbed to the definitions of the corresponding physical quantities and do not have observable effects.

The most notable physical effect is the small electric charge which is approximately $g_X \hat{c}_W t_\varepsilon$ for small ε that the dark fermion χ obtains. This allows scattering of photons to dark photons via $\chi A \leftrightarrow \chi X$ enabling energy flow between the visible and dark sector. In the FIMP scenario, the dark matter density would be generated via annihilations such as $\bar{f}f \to \bar{\chi}\chi$ and $AA \to \bar{\chi}\chi$. However, due to the amplitude being suppressed by two powers of ε these processes have a very small cross section. Thus once a substantial density of dark matter exists, the photon to dark photon scattering becomes significant, having an amplitude suppressed only by one power of ε, which would feed the dark photon density, leading to a significant abundance of dark radiation. If the coupling g_X is assumed to be substantial (~ 0.1), then the dark sector quickly thermalizes. Under the assumption that the dark

matter is of the FIMP type this means that the visible and dark sectors will have separate temperatures T and T_D. The evolution of these temperatures is primarily determined by processes within the two sectors, but the scattering $\chi A \leftrightarrow \chi X$ will seek to drive them towards mutual equilibrium.

In the case that the dark photon X is massive, the couplings of the dark fermion are those given by (4.11). Namely, the visible sector photon is completely uncoupled from the dark matter, and the Z-boson has a small coupling to the dark fermions. Unlike in the case where the dark sector has no fermions, the mass of X is not restricted to be very small since it does not need to be a dark matter candidate. Since the massive dark photon couples to standard model fermions via the Z-esque interaction in (4.6), if $m_X \geq 2m_\chi$, the primary generation processes of dark matter are the coalescence–decay process $\bar{f}f \to X \to \bar{\chi}\chi$, and the annihilation $\bar{f}f \to \bar{\chi}\chi$. In the case the dark photons are much lighter than the fermions, then they can never decay to dark fermions, and the annihilation will solely remain the primary channel. In this case there will be a population of dark photons in the early universe. This population can be stable if the dark photon mass is smaller than the neutrino masses, but in any other case will eventually decay to standard model particles.

5 CONSTRAINTS ON KINETIC MIXING

5.1 Particle physics constraints

As we saw in section 4.1, in some models of kinetic mixing the addition of the dark sector produced observable modifications to the parameters of the theory. In particular, we saw that if the dark photon was massive, it introduced a tree-level correction to the parameter $\rho = m_W^2/m_Z^2 c_W^2$, where m_W and m_Z are the masses from the pole of the propagator, and the weak mixing angle is defined from the Fermi coupling constant. Then if ε is small, and the dark photon mass is much smaller than the Z-boson mass, the ρ parameter gives the bound

$$\rho - 1 = s_W^2 \varepsilon^2$$

With the most recent value $\rho - 1 = \pm 0.00019$ at 68% confidence interval from the Particle Data Group (2018) we see using the approximate value $s_W^2 \approx 0.23$ that $\varepsilon < 0.029$.

Another constraint discussed in section 4.1 was the anomalous magnetic moment which, under the assumption that mixing was small, received a contribution as given in equation (4.12). Getting direct bounds on ε from this is trickier than it was for the ρ-parameter. Constraints from the muon magnetic moment for a generic extra U(1) field have been discussed by Fayet (2007), and in the particular context of kinetic mixing by Chun, Park, and Scopel (2011). Both found bounds which are of the same order of magnitude as the ρ-parameter constraint from small m_X.

For the models where the dark photon is massless, the situation is even worse, since as discussed in section 4.2, the theory without a dark fermion predicts the same values for observables, and with a dark fermion only interactions involving it differ from the standard model. In particular, modifications to the ρ-parameter and magnetic moments only come from loops involving the dark fermion, which constrains the model very poorly.

5.2 Direct detection constraints

Various nuclear recoil based searches of dark matter have placed strong constraints on the model-independent DM–nucleus cross sections. In the kinetic mixing model, the nature of the interaction of the dark fermion with the nucleus varies depending on whether we are working with massive or massless dark photons. Consider first the situation where our target dark matter particle is a dark fermion, and the dark photon assumes the role of a mediator between the visible and the dark sector. Then, if the dark photon is massive, the scattering occurs either via the mediation of a Z-boson or

an X-boson, according to the interaction terms (4.5), (4.6), and (4.11). The axial contribution vanishes in this process, so we have to lowest order in ε the effective interactions

$$\frac{e}{c_W s_W}(s_W^2 + \tfrac{1}{4})\bar{p}\not{Z}p, \quad \frac{e}{4c_W s_W}\bar{n}\not{Z}n, \quad ec_W\varepsilon\bar{p}\not{X}p. \tag{5.1}$$

Note that since $t_\xi + s_W t_\varepsilon = \mathcal{O}(\varepsilon^2)$ the axial coupling of the dark photon to standard model fermions essentially vanishes at lowest order, causing it to effectively have no coupling to uncharged particles. For our purposes, it is useful to write down an effective charge that a nucleus N has with respect to a given vector field such that we can write the interactions of the nucleus as $eQ^Z_{\text{eff}}\bar{N}\not{Z}N + e\varepsilon Q^X_{\text{eff}}\bar{N}\not{X}N$, where

$$Q^Z_{\text{eff}} = \frac{(1+4s_W^2)Z + (A-Z)}{4c_W s_W}, \quad Q^X_{\text{eff}} = c_W Z$$

with Z being the proton number and A being the mass number. The $N\chi \to N\chi$ cross section in the limit of zero momentum transfer to first order in ε can then be written as (Kaplinghat, Tulin, and Yu 2014)

$$\sigma_{\chi N} = 16\pi\mu_{\chi N}^2 \frac{\alpha\alpha_X}{m_X^4}\varepsilon^2((Q^X_{\text{eff}})^2 + 2s_W Q^Z_{\text{eff}}Q^X_{\text{eff}}R_{XZ}^2 + s_W^2(Q^Z_{\text{eff}})^2 R_{XZ}^4),$$

where α is the usual fine structure constant while α_X is the dark fine structure constant, $\mu_{\chi N}$ is the reduced mass of the χN system, and $R_{XZ} = m_X/m_Z$ is the XZ mass ratio. We see that if the dark photon is significantly lighter than the Z-boson, then the interaction occurs primarily via the dark photon, and we have the cross section

$$\sigma_{\chi N} = 16\pi\mu_{\chi N}^2 \alpha c_W^2 Z^2 \frac{\alpha_X\varepsilon^2}{m_X^4}.$$

In particular, for a dark fermion with mass $m_\chi \gg m_p$, we have the approximate χ–proton cross section

$$\sigma_{\chi p} \approx \left(\frac{\text{MeV}}{m_X}\right)^4 \alpha_X\varepsilon^2 \times 10^{-20}\ \text{cm}^2.$$

Assuming the recent DarkSide-50 bounds on the DM–Nucleon cross section in the above range (DarkSide Collaboration 2018), we have the limit

$$\left(\frac{\text{MeV}}{m_X}\right)^2 \alpha_X^{1/2}\varepsilon < 10^{-10}.$$

If in turn the mass of the dark fermion is significantly below the proton mass, then $\mu_{\chi p} \approx m_\chi$, and we have

$$\frac{m_\chi}{m_p}\left(\frac{\text{MeV}}{m_X}\right)^2 \alpha_X^{1/2}\varepsilon < 10^{-10}.$$

Since this expression was derived in the limit of zero momentum transfer, it is invalid for dark photon masses significantly less than the kinetic energies of typical dark matter particles.

When it comes the model with massless dark photons, we can use the choice of basis picked in section 4.3 in which the dark photon X decouples and interactions of dark fermions with standard model particles are essentially electromagnetic in nature. This means that the χ-nucleus can in the limit of small ε be modeled as the scattering of a charged fermion of charge $-g_X c_W \varepsilon/e$ off the nucleus, which in the nonrelativistic limit leads to Coulomb scattering. While the Coulomb scattering cross section is formally infinite, the pole that produces the infinite cross section arises from the zero momentum transfer limit while the momentum transfer that can be detected is in reality limited by the sensitivity of the detector. For discussion of the direct detection bounds a proper regularization of the cross section is needed.

Finally, we may consider the possibility where the dark matter particle is the massive dark photon itself. The relevant scattering in this case is essentially Compton scattering of a massive vector boson off a fermion. The relevant interaction here is the last term of (5.1) which gives the interaction between the proton and the dark photon. However, the amplitude for the proper scattering amplitude $\mathcal{A}(pX \to pX)$ is suppressed by two powers of ε, which makes the scattering cross section quartic in ε. The lowest order interaction between the nucleus and the dark photon, is the absorption $pX \to p$. The amplitude for this process is essentially the same as the dark photon production amplitude, and so the scattering cross section is

$$\sigma(pX \to p) = \frac{2\pi^2}{3} \frac{\alpha c_W^2 m_p}{E_X p_X} \varepsilon^2 \left(2 + \frac{m_X^2}{m_p^2}\right) \delta(E_p - E_X).$$

Here E_X and p_X are the energy and the momentum of the incoming dark photon, while E_p is the energy of the outgoing proton. The delta function comes from energy conservation, and in practice one must integrate over the thermal distribution of dark photons to get theoretical estimates to be compared with data.

5.3 Astrophysical constraints

Dark sector particles can be produced from visible sector particles via a variety of channels. Due to the small coupling between the sectors, this production rate is only significant in a sufficiently dense plasma over sufficiently long time periods, which is why the cosmological effects in the early universe are of prime interest. However, the dense cores of stars provide another environment where relatively large quantities of dark matter may be produced. While the rate of this prediction is too low to have a meaningful impact on the expected abundance of dark matter, because the dark matter that has been generated inside the star is unlikely to be reabsorbed on its way out, it is expected to contribute to stellar cooling. Since stellar evolution is a well studied phenomenon, it can offer meaningful constraints on dark matter.

While the interaction of the dark photons with ground based detectors is weak, it is also possible that some of the helioscope experiments intended for detecting axion production in the sun could be sensitive enough to constrain dark photons.

The production of dark photons can be expected to occur in a transfer of energy from the photon gas inside the cores of stars to the dark photons via Compton scattering type reactions $f\gamma \to fX$ where a photon scatters into a dark photon, as well as an emission type process $i \to fX$ where an initial state particle decays into a dark photon and a final state. The production of light dark photons inside stars has been studied by Redondo (2008) as well as An, Pospelov, and Pradler (2013) in a simpler case where the dark photon mixes with the electromagnetic field strength $F_{\mu\nu}$ rather than with the hypercharge $B_{\mu\nu}$.

5.4 Cosmological constraints

The interactions of the dark matter with the visible sector naturally affect the evolution of visible sector matter densities, which gives rise to a variety of cosmological observables that can be used to constrain the dark matter. In this section we discuss some of the cosmological constraints on the different kinetic mixing models.

As discussed previously, when the dark photon has a mass, it has a decay channel to the visible sector which allows for energy injection into and consequent heating of baryons. The rate of energy injection from decays can be written as

$$K_X = \zeta m_b \Gamma_X e^{-\Gamma_X t},$$

in accordance with Zhang et al. (2007) using the conventions of Fradette et al. (2014) where $\zeta = f\Omega_X/\Omega_b$, with m_b the baryon mass, Ω_X and Ω_b the respective density parameters of dark photons and baryons today, Γ the decay rate, and f a factor related to the efficiency of energy injection. The injection of energy from particle decays after recombination leaves an imprint on the CMB by enhancing the TE and EE power spectra on small scales, while damping the TT spectrum at large scales (Zhang et al. 2007; Slatyer, Padmanabhan, and Finkbeiner 2009). If the lifetime is longer than the age of the universe—as is required by dark matter made of dark photons—then the exponential factor in K_X is unity. The CMB then sets bounds on the quantity $\zeta\Gamma_X$, which can be translated to the model parameters ε and m_X since

$$\zeta = \frac{m_X}{m_b}\frac{Y_{X0}}{Y_{b0}},$$

where $Y = n/s$ is the number density to entropy ratio today, and Γ_{X0} can be solved from the Boltzmann equation as a function of (ε, m_X).

Note that the above bound only applies when the decay is slow and the creation rate of dark photons can be neglected. In the general case, if the dark sector contains fermions χ with $m_X > 2m_\chi$, the dark photons can rapidly

decay into fermions. However, if they are assumed light relative to the fermions, then the above bound remains applicable.

Apart from late time injection of energy after recombination, reactions between the dark and visible sectors can also inject energy and particles to the visible sector at the time of the Big Bang nucleosynthesis (BBN), which can impact a variety of BBN predictions. For one, the abundances of various light elements are altered. This is a particularly interesting bound in the context of the lithium problem—the discrepancy between the observed ratio of ^{7}Li/H, and the ratio predicted by standard BBN which is two to three times higher(Cyburt, Fields, and Olive 2008)—since it is known that injection of extra neutrons helps transforms ^{7}Be to ^{7}Li, reducing the final abundance of ^{7}Li, and such a neutron injection can be brought about by decays of a massive particle (Reno and Seckel 1988; Jedamzik 2004; Pospelov and Pradler 2010). Of course, useful bounds also result from the effect of decays on abundance of other light elements.

The BBN is also sensitive to the amount of radiation in the universe at $T \sim 1$ MeV. Therefore if there exists a new particle species which is relativistic at the time of BBN, such as a low-mass or even massless dark photon, its presence will impact the predictions of BBN. Namely, the effects of radiation are parametrized by the effective number of relativistic degrees of freedom $g_*(T \sim 1 \text{ MeV})$ at the time of BBN. If we have a dark sector which is out of equilibrium with the visible sector, but is internally at equilibrium with a temperature T_D (note that this requires more structure than the single dark photon in the dark sector), then the total number of radiation degrees of freedom splits as

$$g_*(T) = g_{*\text{SM}}(T) + g_{*\text{D}}(T_\text{D}/T).$$

The modification to the number of relativistic degrees of freedom at the time of BBN is usually parametrized by the effective number of neutrino species N_ν. The addition of dark photons can then be characterized as a modification δN_ν to N_ν such that $g_*(T) = g_{*\text{SM}}(T) + \frac{7}{4}\delta N_\nu$. The quantity N_ν is a well constrained by data with the Planck Collaboration (2018) giving $N_\nu \leq 3.33$ at 95% confidence. This bound will be discussed in detail in the next section.

5.5 The constraints from N_ν

As mentioned at the end of the previous section, the presence of dark photons introduces extra relativistic degrees of freedom, which impact the BBN and are experimentally parametrized by the effective number of neutrino species N_ν. In this section we study how this constrains kinetic mixing dark matter in the specific case where there exists a dark fermion χ and the dark photons are massless. The methods discussed here are based on the work of Cline et al. (2014). It is worth noting that for this bound to give anything interesting, the dark sector needs to have more structure than the single dark photon since the dark photons interact too weakly to thermalize, or if they thermalize, they necessarily thermalize to the visible sector temperature T. To get nontrivial bounds, we need a thermal distribution of dark photons with a temperature

different from that of the visible sector, which means a dark sector particle with which the dark photons interact relatively strongly with respect to their interactions with the visible sector.

The assumption that the dark photon is massless and not an extremely light particle most crucially means that it has two spin degrees of freedom rather than three. Thus equating its contribution $2(T_{\mathrm{D}}/T)^4$ to $g_*(T)$ with the contribution from effective neutrino species gives the relation

$$\frac{T_{\mathrm{D}}}{T} = (\tfrac{7}{8}\delta N_\nu)^{1/4}$$

between the dark sector temperature T_{D} and the visible sector temperature T. The dark fermion also contributes to the total number of degrees of freedom. However, we assume that its mass m_χ is much larger than the temperature $T \sim 1$ MeV at the time of BBN so that it has long since ceased to be relativistic at the time when N_ν freezes out, as well as that T_D at the time of BBN is not too much higher than T. This latter assumption is well justified since even a relatively modest difference such as $T_{\mathrm{D}}/T \geq 1.5$ requires $\delta N_\nu \geq 5.7$ which is well ruled out by observations.

In order to find the temperature ratio T_D/T at the time of BBN, we may first relate the temperatures to the densities of the respective photons. Thus by (2.6) we have

$$\zeta = \frac{T_{\mathrm{D}}}{T} = \left(\frac{\rho_X}{\rho_\gamma}\right)^{1/4}.$$

We then use the Boltzmann equations

$$\dot{\rho}_\gamma + 4H\rho_\gamma = q_{\mathrm{SM}} - q_s, \quad \dot{\rho}_X + 4H\rho_X = q_{\mathrm{D}} + q_s, \tag{5.2}$$

to solve the densities with the appropriate initial conditions. Here q_{SM} is a collision term from interactions of the photon gas with standard model particles, q_{D} is a similar collision term for interactions between the dark photons and dark fermions, while q_s is a term that allows exchange of energy between the two sectors.

Before discussing the specifics of the collision terms in the above equations, we should consider the appropriate initial conditions. In the FIMP scenario the dark sector starts unoccupied, implying $T_D = 0$. However, implementing this initial condition would require tracking the reactions that fill the dark sector. We will follow the assumption of Cline et al. (2014) that at some sufficiently early time $T_{\mathrm{D}} = T$, which should work provided that ε is not too small. Therefore we will use $T_{\mathrm{D}} = T \sim 1$ GeV as the initial conditions.

When it comes to the collision terms, expressions for the collision terms q_{SM} and q_{D} can be derived from the conservation of entropy. That is, the entropy temperature relation $s \propto g_{*S}(T)T^3$ implies

$$\frac{ds}{dT} = 3sT^{-1}\left(1 + \frac{1}{3}\frac{T}{g_{*S}}\frac{dg_{*S}}{dT}\right).$$

Combining this with the entropy conservation equation $\dot{s} + 3Hs = 0$ allows us to write

$$\frac{\dot{T}}{T} = -H\left(1 - \frac{\frac{1}{3}\frac{T}{g_{*S}}\frac{dg_{*S}}{dT}}{1 + \frac{1}{3}\frac{T}{g_{*S}}\frac{dg_{*S}}{dT}}\right).$$

This can then be plugged into the radiation relation

$$\frac{\dot{\rho}}{\rho} = 4\frac{\dot{T}}{T}.$$

Relating the result with the appropriate Boltzmann equations in the limit where the two sectors are decoupled ($q_s = 0$) then gives

$$q_{\mathrm{SM}} = \frac{4}{3}H\rho_\gamma \frac{\frac{1}{3}\frac{T}{g_*}\frac{dg_{*\mathrm{SM}}}{dT}}{1 + \frac{1}{3}\frac{T}{g_{*\mathrm{SM}}}\frac{dg_{*\mathrm{SM}}}{dT}}, \quad q_{\mathrm{D}} = \frac{4}{3}H\rho_X \frac{\frac{1}{3}\frac{T_{\mathrm{D}}}{g_{*D}}\frac{dg_{*D}}{dT_{\mathrm{D}}}}{1 + \frac{1}{3}\frac{T_{\mathrm{D}}}{g_{*\mathrm{D}}}\frac{dg_{*\mathrm{D}}}{dT_{\mathrm{D}}}}.$$

Here we have taken advantage of the fact that to a good approximation $g_{*S} = g_*$ in the relevant temperature range. Since we are only dealing with temperatures $T \gtrsim 1$ MeV, we write $g_*(T) = 10.75 + g_{*\mathrm{h}}(T)$, where $g_{*\mathrm{h}}(T)$ is the hadronic contribution. We use the parametrization given by Borsányi et al. (2010) for its computation. For $g_{*\mathrm{D}}$ we have to integrate the full integral (2.3) for χ at every temperature since we are dealing with a wide range of possible values for m_χ.

The term q_s includes all exchanges of energy between visible and dark photons. Since we are working in the basis where the dark photons are decoupled from visible fermions, the primary exchange process is the Compton type scattering $\chi\gamma \leftrightarrow \chi X$. Thus we can rely on the two-to-two scattering formula (2.17). This formula is for the collision term of the Boltzmann equation of the number density. However, the relations $\rho/n \propto T$ and $\dot{\rho}/\rho = 4\dot{T}/T$ can be used to relate the two Boltzmann equations. It is then a straightforward consequence that if c is the number density collision term, the relevant collision term for energy density is given by $q = \frac{4}{3}cT^{-1}$ such that

$$q_s = \frac{4}{3}n_\chi(\langle\sigma v\rangle_{\gamma\to X}\rho_\gamma - \langle\sigma v\rangle_{X\to\gamma}\rho_X)$$

Here σ is the full relativistic Compton cross section in the lab frame, which can be expressed in the form $\sigma = \sigma_{\mathrm{T}}\beta(w)/w$, where

$$\beta(w) = \frac{3}{4}\left(\frac{2}{w} + \left(\frac{1}{2} - \frac{1}{w} - \frac{1}{w^2}\right)\ln(1+2w) + \frac{w(1+w)}{(1+2w)^2}\right),$$
$$\sigma_{\mathrm{T}} = \frac{8\pi}{3}\left(\frac{c_W}{m_\chi}\alpha_X\varepsilon\right)^2,$$

with $w = E_{\mathrm{in}}/m_\chi$ and E_{in} the energy of the incoming (dark) photon. Denoting $B(z) = \int \beta(z)\,dz$, the thermally averaged cross sections can then be written

as

$$\langle \sigma v \rangle_{\gamma \to X} = \frac{\sigma_T m_\chi^4 \int f_\chi f_\gamma (B(b) - B(a))\, dE_\gamma\, dE_\chi}{4\zeta(3) T^3 T_D^3 H_1(x)},$$
$$\langle \sigma v \rangle_{X \to \gamma} = \frac{\sigma_T m_\chi^4 \int f_\chi f_\gamma (B(b) - B(a))\, dE_X\, dE_\chi}{4\zeta(3) T_D^6 H_1(x)},$$

where

$$a = \frac{E_{\gamma/X}}{m_\chi^2}(E_\chi - p_\chi), \quad b = \frac{E_{\gamma/X}}{m_\chi^2}(E_\chi + p_\chi); \quad H_1(x) = x^3 \int_1^\infty \frac{\sqrt{t^2-1}}{e^{xt}+1} t\, dt, \tag{5.3}$$

and $x = m_\chi / T_\mathrm{D}$. Derivations of these formulae can be found in appendix A. In the numerical integration of the Boltzmann equations (5.2), the double integral in $\langle \sigma v \rangle$ forms a significant obstacle for fast integration. Fortunately, however, when we write the integral in terms of x and $\zeta \equiv T_\mathrm{D}/T$, all explicit dependence on m_χ falls out which allows us to precompute $\langle \sigma v \rangle$ for a wide range of (x, ζ) and quickly interpolate values during integration.

In figure 5.1 we see the behavior of ζ as a function of $\alpha_X \varepsilon$ for various values of m_χ, where a few notable observations can be made. First, for sufiicciently small values of $\alpha_X \varepsilon$ the parameter ζ plateaus at some value less than unity, and eventually plateaus at unity for sufficiently high $\alpha_X \varepsilon$. For $m_\chi < 1$ MeV the plateau for small couplings is at about $\zeta = 0.59$, and rises from there until for high enough m_χ it s at $\zeta = 0.82$. For 1 MeV $< m_\chi <$ 500 MeV the value of ζ peaks above unity for some range of couplings, and for $m_\chi > 600$ MeV the value of ζ dips down before peaking.

Previous constraints from the era of WMAP data are too weak to constrain ζ below unity. The present day constraints from Planck data set $\delta N_\nu < 0.284$ at 95% confidence level, which corresponds to $\zeta < 0.71$. This not only excludes all values of ζ above unity, but also below the magic value of 0.84 where all masses between 3 MeV and 1 GeV become excluded for arbitrarily small couplings. Furthermore, for $m_\chi < 1$ GeV all FIMP scale couplings $\alpha_X \varepsilon$ above 4×10^{-11} are excluded. In conclusion, the best present day constraint $\zeta < 0.71$ excludes large portions of $(m_\chi, \alpha_X \varepsilon)$-plane as seen in figure 5.2.

It is worth keeping in mind, however, the range of validity of the above analysis. In particular, we assumed that the abundance of χ has been frozen at least since $T \sim 1$ GeV, which requires ε to be small enough. Furthermore, the initial condition $T_D = T$ used requires ε to be large enough that a sufficient density is generated in the dark sector. This is why, in particular, the total exclusion of masses > 3 MeV should not be taken too seriously. With initial conditions appropriate for arbitrarily small ε the dark sector is expected to end up much colder for decreasing ε.

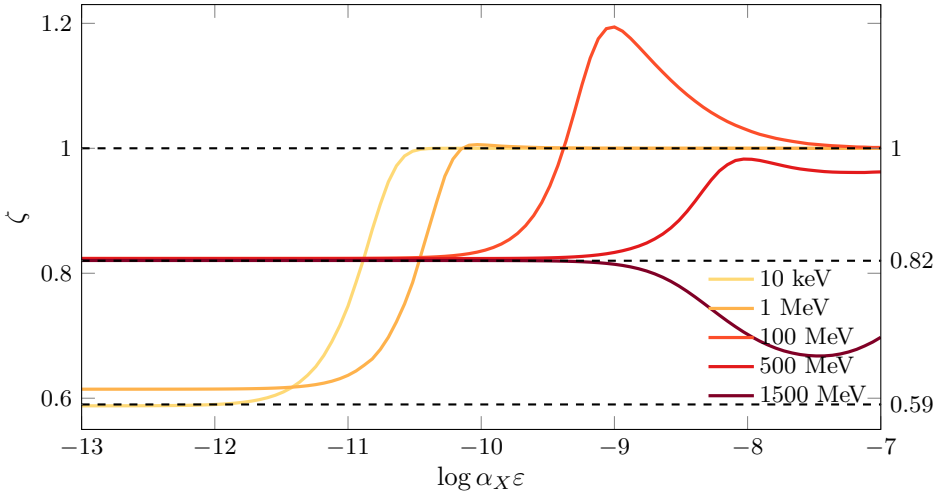

Figure 5.1: The behavior of $\zeta = T_\mathrm{D}/T$ at BBN as a function of the coupling $\alpha_X \varepsilon$ for various masses. few notable asymptotic values of ζ are included. The bound $\zeta < 0.82$ completely excludes all masses m_χ between 3 MeV and 1 GeV. Managing to constrain $\zeta < 0.59$ would be enough to completely exclude all sufficiently small (below 1 GeV) masses in this approximation.

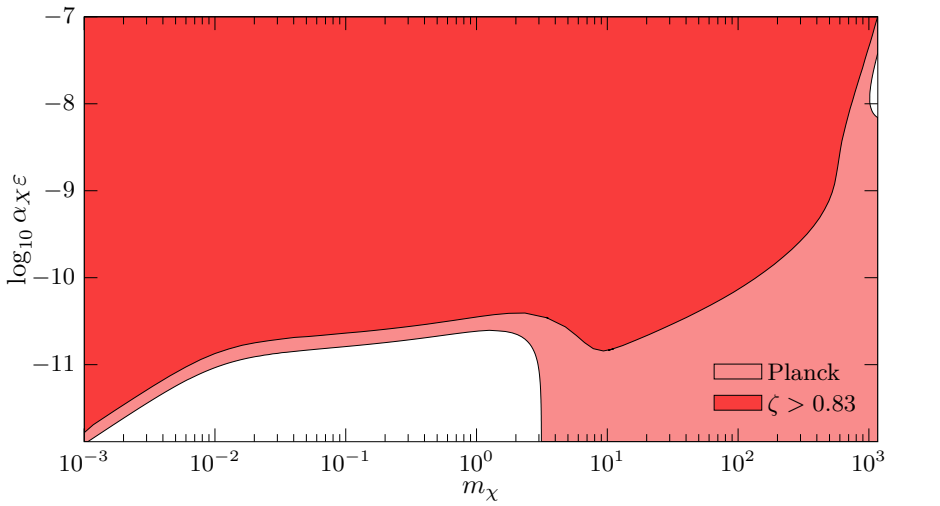

Figure 5.2: The parts of the (m_χ, α_x)-plane excluded by the N_ν bound. Light red marks the part of the plane excluded by the Planck Collaboration (2018) 95% confidence level bound $N_\nu < 3.33$ for Planck + BAO. The area with $\zeta > 0.83$ is shown for comparison with darker red.

6 CONCLUSIONS

Kinetic mixing offers a wide range of possible models for dark matter from a massive photon being the sole dark matter particle to a dark sector with multiple types of particles forming all kinds of bound states. The case of the massless dark photon in particular raises some interesting theoretical questions, since the O(2) ambiguity in defining what is the usual photon and what is the dark photon field creates some nontrivial questions of what is observable and what is not observable in the theory. If one accepts that all experiments in reality only involve fermions in the final state when the experimental apparatus is taken into consideration, and thus cannot make a distinction between photons and massless dark photons, one is faced with the result that the introduction of an extra unbroken U(1) symmetry to the standard model by itself does not lead to observable changes in the parameters of the theory.

From the theory of kinetic mixing some usable bounds which are testable by direct collider experiments can be obtained, but these bounds unfortunately do not appear to be strict enough to be applicable to FIMP scale interactions in the near future, and in any case only exist for the massive dark photon. Modern direct detection constraints are coming close to giving useful bounds also in the FIMP regime, but there the specifics of the dark sector such as the strength of interactions within the dark sector and the masses of the dark fermions come into play, leading to a larger parameter space. In the domain of cosmological constraints, modern bounds on the effective number of neutrino degrees of freedom manage to close a significant portion of the FIMP parameter space for a model with a massless dark photon and a single dark fermion which couples to itself sufficiently strongly via the dark photon. However, introduction of a dark photon mass and additional fermions into the dark sector could change the physics drastically. The effects of giving the dark photon a small mass $m_X \ll 1$ MeV are also not known. More study would be needed to determine the robustness of the bound under changes in contents of the dark sector.

A DERIVATION OF THE THERMALLY AVERAGED CROSS SECTION FOR COMPTON SCATTERING

The $\chi\gamma \leftrightarrow \chi X$ scattering is in practice just Compton scattering, so we can start from the spin averaged square of the ampltiude with the correct coupling

$$\frac{1}{4}\sum |\mathcal{M}|^2 =$$
$$2(g_X^2 \varepsilon c_W)^2 \left(\frac{q\cdot p'}{q\cdot p} + \frac{q\cdot p}{q\cdot p'} + 2m_{e'}^2 \left(\frac{1}{q\cdot p} - \frac{1}{q\cdot p'} \right) + m_{e'}^4 \left(\frac{1}{q\cdot p} - \frac{1}{q\cdot p'} \right)^2 \right)$$

Here p and p' are the momenta of the incoming and outgoing (dark) photons respectively, and q is the momentum of the incoming χ. This expression is most straightforwardly simplified by first going to the lab frame where the χ is stationary. Then using the famous equation

$$\frac{E_{\text{out}}}{E_{\text{in}}} = \frac{1}{1 + \frac{E_{\text{in}}}{m_\chi}(1-\cos\theta)},$$

and letting $w = E_{\text{in}}/m_\chi$ and $y = 1 - \cos\theta$, we have

$$\frac{1}{4}\sum |\mathcal{M}|^2 = 2(g_X^2 \varepsilon c_W)^2 \left(\frac{1}{1+wy} + 1 + wy - y(2-y) \right).$$

For this, the relativistically invariant cross section defined in (2.16) can be written as

$$\sigma = \frac{(g_X^2 \varepsilon c_W)^2}{16\pi m_\chi^2} \int_0^2 \frac{1}{(1+wy)^2} \left(\frac{1}{1+wy} + 1 + wy - y(2-y) \right) dy.$$

A straightforward integration then gives

$$\sigma = \frac{(g_X^2 s_\varepsilon c_W)^2}{16\pi m_{e'}^2} \frac{1}{w} \left(\frac{4}{w} + \left(1 - \frac{2}{w} - \frac{2}{w^2} \right) \ln(1+2w) + 2w \frac{1+w}{(1+2w)^2} \right) \quad \text{(A.1)}$$

We then note that in the lab frame $w = \frac{1}{2}(s/m_\chi^2 - 1)$, where s is the Mandelstam variable $(p+q)^2$. With s and σ relativistically invariant, (A.1) then holds in all frames, with the understanding that $w = \frac{1}{2}(s/m_\chi^2 - 1)$. At this point we define $\sigma = \sigma_{\text{T}}\beta(w)/w$, where

$$\sigma_{\text{T}} = \frac{8}{3}\frac{(g_X^2 s_\varepsilon c_W)^2}{16\pi m_{e'}^2} = \frac{8\pi}{3}\left(\frac{\alpha' s_\varepsilon c_W}{m_{e'}} \right)^2, \quad \alpha' = \frac{g_X}{4\pi},$$

and

$$\beta(w) = \frac{3}{4}\left(\frac{2}{w} + \left(\frac{1}{2} - \frac{1}{w} - \frac{1}{w^2}\right)\ln(1+2w) + w\frac{1+w}{(1+2w)^2}\right).$$

We can now write down the thermally averaged cross section

$$\langle\sigma v\rangle = \frac{\int f_\chi f_i \sigma v \, d^3p \, d^3q}{\int f_i \, d^3p \int f_\chi \, d^3q}$$

where v is the Møller velocity $v = F/E_pE_q$ as defined in section 2.2. Here i stands for either γ or X, depending on which scattering direction we are considering. The first integral in the denominator is a standard integral $\int f_i \, d^3p = 4\pi\Gamma(3)\zeta(3)T_i^3$, with ζ the Riemann zeta function, and T_i is either T or T_D again depending on the scattering direction. The second integral in the denominator has no analytic solution. We define

$$H_1(x) = \int_x^\infty \frac{\sqrt{u^2 - x^2}}{e^u + 1} u \, du,$$

and write $\int f_\chi \, d^3q = 4\pi T_\mathrm{D}^3 H_1(x)$, where $x = m_\chi/T_D$. The numerator immediately simplifies to

$$8\pi^2 \int f_\chi f_i \sigma F E_p q \, dE_p \, dE_q \, d\cos\theta,$$

with $\cos\theta$ the angle between $\boldsymbol{p}$ and $\boldsymbol{q}$. The only θ-dependent quantity here is σF, and so we can deal with $\int \sigma F \, d\cos\theta$ independently. We can make a change of variables to w using the relation $E_p(E_q - q\cos\theta) = m_\chi^2 w$. The limits of integration are recovered from $|\cos\theta| < 1$, and are

$$a = \frac{E_p}{m_\chi^2}(E_q - q) < w < \frac{E_p}{m_\chi^2}(E_q + q) = b.$$

Then

$$\int \sigma F \, d\cos\theta = \sigma_T \frac{m_\chi^4}{qE_p} \int_a^b \beta(w) \, dw = \sigma_T \frac{m_\chi^4}{qE_p}(B(b) - B(a)),$$

where $B(w) = \int \beta(w) \, dw$. The integral $\int \beta(w) \, dw$ is analytically solvable and can eventually be written as

$$B(w) = \frac{3}{16}(1+2w)\left[\left(1 + \frac{4}{w}\right)\ln(1+2w) - 2\frac{w(1+w)}{(1+2w)^2}\right] + \frac{3}{4}\,\mathrm{Li}_2(-2w),$$

where Li_2 is the dilogarithm function

$$\mathrm{Li}_2(z) = -\int_0^z \frac{\ln(1-x)}{x} \, dx.$$

Thus we have

$$\langle\sigma v\rangle = \frac{\sigma_T m_\chi^4 \int f_\chi f_i (B(b) - B(a)) \, dE_i \, dE_\chi}{4\zeta(3) T_i^3 T_\mathrm{D}^3 H_1(x)} \tag{A.2}$$

BIBLIOGRAPHY

Aalseth, C. E., P. S. Barbeau, J. Colaresi, et al. (Jan. 2014). "Search for An Annual Modulation in Three Years of CoGeNT Dark Matter Detector Data". In: *arXiv e-prints*, arXiv:1401.3295. arXiv: 1401.3295 [astro-ph.CO].

An, Haipeng, Maxim Pospelov, and Josef Pradler (Oct. 2013). "New stellar constraints on dark photons". In: *Physics Letters B* 725, pp. 190–195. DOI: 10.1016/j.physletb.2013.07.008. arXiv: 1302.3884 [hep-ph].

Angloher, G., M. Bauer, I. Bavykina, et al. (Apr. 2012). "Results from 730 kg days of the CRESST-II Dark Matter search". In: *European Physical Journal C* 72, 1971, p. 1971. DOI: 10.1140/epjc/s10052-012-1971-8. arXiv: 1109.0702 [astro-ph.CO].

Angloher, G., A. Bento, C. Bucci, et al. (Dec. 2014). "Results on low mass WIMPs using an upgraded CRESST-II detector". In: *European Physical Journal C* 74, 3184, p. 3184. DOI: 10.1140/epjc/s10052-014-3184-9. arXiv: 1407.3146 [astro-ph.CO].

Ata, Metin, Falk Baumgarten, Julian Bautista, et al. (Feb. 2018). "The clustering of the SDSS-IV extended Baryon Oscillation Spectroscopic Survey DR14 quasar sample: first measurement of baryon acoustic oscillations between redshift 0.8 and 2.2". In: *Monthly Notices of the Royal Astronomical Society* 473, pp. 4773–4794. DOI: 10.1093/mnras/stx2630. arXiv: 1705.06373 [astro-ph.CO].

Athanassoula, E., A. Bosma, and S. Papaioannou (June 1987). "Halo parameters of spiral galaxies". In: *Astronomy and Astrophysics* 179, pp. 23–40.

Begeman, K. G., A. H. Broeils, and R. H. Sanders (Apr. 1991). "Extended rotation curves of spiral galaxies – Dark haloes and modified dynamics". In: *Monthly Notices of the Royal Astronomical Society* 249, pp. 523–537. DOI: 10.1093/mnras/249.3.523.

Bernabei, Rita, Pierluigi Belli, Andrea Bussolotti, et al. (Nov. 2018). "First Model Independent Results from DAMA/LIBRA–Phase2". In: *Universe* 4, p. 116. DOI: 10.3390/universe4110116. arXiv: 1805.10486 [hep-ex].

Bernal, Nicolás, Matti Heikinheimo, Tommi Tenkanen, et al. (Sept. 2017). "The dawn of FIMP Dark Matter: A review of models and constraints". In: *International Journal of Modern Physics A* 32, 1730023-274. DOI: 10.1142/S0217751X1730023X. arXiv: 1706.07442 [hep-ph].

Bertone, Gianfranco and Dan Hooper (May 2016). "A History of Dark Matter". In: *arXiv e-prints*, arXiv:1605.04909. arXiv: 1605.04909 [astro-ph.CO].

Borsányi, Szabolcs, Gergely Endrdi, Zoltán Fodor, et al. (Nov. 2010). "The QCD equation of state with dynamical quarks". In: *Journal of High Energy*

Physics 2010, 77, p. 77. DOI: 10.1007/JHEP11(2010)077. arXiv: 1007.2580 [hep-lat].

Brooks, A. M., M. Kuhlen, A. Zolotov, et al. (Mar. 2013). "A Baryonic Solution to the Missing Satellites Problem". In: *The Astrophysical Journal* 765, 22, p. 22. DOI: 10.1088/0004-637X/765/1/22. arXiv: 1209.5394.

CDMS Collaboration (Apr. 2013). "Silicon Detector Dark Matter Results from the Final Exposure of CDMS II". In: *arXiv e-prints*, arXiv:1304.4279. arXiv: 1304.4279 [hep-ex].

Cheung, Kingman and Tzu-Chiang Yuan (Mar. 2007). "Hidden fermion as milli-charged dark matter in Stueckelberg Z' model". In: *Journal of High Energy Physics* 2007, 120, p. 120. DOI: 10.1088/1126-6708/2007/03/120. arXiv: hep-ph/0701107 [hep-ph].

Chun, Eung Jin, Jong-Chul Park, and Stefano Scopel (Feb. 2011). "Dark matter and a new gauge boson through kinetic mixing". In: *Journal of High Energy Physics* 2011, 100, p. 100. DOI: 10.1007/JHEP02(2011)100. arXiv: 1011.3300 [hep-ph].

Cline, James M., Zuowei Liu, Guy D. Moore, et al. (July 2014). "Composite strongly interacting dark matter". In: *Physical Review D* 90, 015023, p. 015023. DOI: 10.1103/PhysRevD.90.015023. arXiv: 1312.3325 [hep-ph].

Clowe, Douglas, Marua Brada, Anthony H. Gonzalez, et al. (Aug. 2006). "A Direct Empirical Proof of the Existence of Dark Matter". In: *The Astrophysical Journal* 648.2, pp. L109–L113. DOI: 10.1086/508162. URL: https://doi.org/10.1086%2F508162.

Colín, Pedro, Vladimir Avila-Reese, and Octavio Valenzuela (Oct. 2000). "Substructure and Halo Density Profiles in a Warm Dark Matter Cosmology". In: *The Astrophysical Journal* 542.2, pp. 622–630. DOI: 10.1086/317057. URL: https://doi.org/10.1086%2F317057.

Cyburt, Richard H., Brian D. Fields, and Keith A. Olive (Nov. 2008). "An update on the big bang nucleosynthesis prediction for ^{7}Li: the problem worsens". In: *Journal of Cosmology and Astroparticle Physics* 2008, 012, p. 012. DOI: 10.1088/1475-7516/2008/11/012. arXiv: 0808.2818 [astro-ph].

Cyr-Racine, Francis-Yan and Kris Sigurdson (May 2013). "Cosmology of atomic dark matter". In: *Physical Review D* 87, 103515, p. 103515. DOI: 10.1103/PhysRevD.87.103515. arXiv: 1209.5752 [astro-ph.CO].

DarkSide Collaboration (Feb. 2018). "Low-Mass Dark Matter Search with the DarkSide-50 Experiment". In: *arXiv e-prints*, arXiv:1802.06994. arXiv: 1802.06994 [astro-ph.HE].

de Blok, W. J. G. (Jan. 2010). "The Core-Cusp Problem". In: *Advances in Astronomy* 2010, 789293, p. 789293. DOI: 10.1155/2010/789293. arXiv: 0910.3538 [astro-ph.CO].

DES Collaboration (Nov. 2015). "Eight Ultra-faint Galaxy Candidates Discovered in Year Two of the Dark Energy Survey". In: *The Astrophysical Journal* 813, 109, p. 109. DOI: 10.1088/0004-637X/813/2/109. arXiv: 1508.03622 [astro-ph.GA].

Dubinski, J. and R. G. Carlberg (Sept. 1991). "The structure of cold dark matter halos". In: *The Astrophysical Journal* 378, pp. 496–503. DOI: 10.1086/170451.

Einasto, Jaan, Ants Kaasik, and Enn Saar (July 1974). "Dynamic evidence on massive coronas of galaxies". In: *Nature* 250, pp. 309–310. DOI: 10.1038/250309a0. URL: https://doi.org/10.1038/250309a0.

Elbert, O. D., J. S. Bullock, S. Garrison-Kimmel, et al. (Oct. 2015). "Core formation in dwarf haloes with self-interacting dark matter: no fine-tuning necessary". In: *Monthly Notices of the Royal Astronomical Society* 453, pp. 29–37. DOI: 10.1093/mnras/stv1470. arXiv: 1412.1477.

Fayet, Pierre (June 2007). "U-boson production in e^+e^- annihilations, ψ and Υ decays, and light dark matter". In: *Physical Review D* 75, 115017, p. 115017. DOI: 10.1103/PhysRevD.75.115017. arXiv: hep-ph/0702176 [hep-ph].

Feldman, Daniel, Zuowei Liu, and Pran Nath (June 2007). "Stueckelberg $Z^{'}$ extension with kinetic mixing and millicharged dark matter from the hidden sector". In: *Physical Review D* 75, 115001, p. 115001. DOI: 10.1103/PhysRevD.75.115001. arXiv: hep-ph/0702123 [hep-ph].

Fradette, Anthony, Maxim Pospelov, Josef Pradler, et al. (Aug. 2014). "Cosmological constraints on very dark photons". In: *Physical Review D* 90, 035022, p. 035022. DOI: 10.1103/PhysRevD.90.035022. arXiv: 1407.0993 [hep-ph].

Galison, P. and A. Manohar (Mar. 1984). "Two Z's or not two Z's?" In: *Physics Letters B* 136, pp. 279–283. DOI: 10.1016/0370-2693(84)91161-4.

Goldberg, H. and L. J. Hall (July 1986). "A new candidate for dark matter". In: *Physics Letters B* 174, pp. 151–155. DOI: 10.1016/0370-2693(86)90731-8.

Gondolo, P. and G. Gelmini (Aug. 1991). "Cosmic abundances of stable particles: improved analysis." In: *Nuclear Physics B* 360, pp. 145–179. DOI: 10.1016/0550-3213(91)90438-4.

Governato, F., A. Zolotov, A. Pontzen, et al. (May 2012). "Cuspy no more: how outflows affect the central dark matter and baryon distribution in Λ cold dark matter galaxies". In: *Monthly Notices of the Royal Astronomical Society* 422, pp. 1231–1240. DOI: 10.1111/j.1365-2966.2012.20696.x. arXiv: 1202.0554 [astro-ph.CO].

Gunn, J. E., B. W. Lee, I. Lerche, et al. (Aug. 1978). "Some astrophysical consequences of the existence of a heavy stable neutral lepton". In: *The Astrophysical Journal* 223, pp. 1015–1031. DOI: 10.1086/156335.

Hall, Lawrence J., Karsten Jedamzik, John March-Russell, et al. (Mar. 2010). "Freeze-in production of FIMP dark matter". In: *Journal of High Energy Physics* 2010, 80. DOI: 10.1007/JHEP03(2010)080. arXiv: 0911.1120 [hep-ph].

Hernquist, Lars, Neal Katz, David H. Weinberg, et al. (Feb. 1996). "The Lyman-Alpha Forest in the Cold Dark Matter Model". In: *The Astrophysical Journal* 457.2. DOI: 10.1086/309899. URL: https://doi.org/10.1086%2F309899.

Hewett, JoAnne L. and Thomas G. Rizzo (1989). "Low-energy phenomenology of superstring-inspired E_6 models". In: *Physics Reports* 183.5, pp. 193–381. ISSN: 0370-1573. DOI: https://doi.org/10.1016/0370-1573(89)90071-9. URL: http://www.sciencedirect.com/science/article/pii/0370157389900719.

Hoekstra, H., M. Bartelmann, H. Dahle, et al. (Aug. 2013). "Masses of Galaxy Clusters from Gravitational Lensing". In: *Space Science Reviews* 177, pp. 75–118. DOI: 10.1007/s11214-013-9978-5. arXiv: 1303.3274.

Holdom, Bob (1986). "Two U(1)'s and ε charge shifts". In: *Physics Letters B* 166.2, pp. 196–198. ISSN: 0370-2693. DOI: https://doi.org/10.1016/0370-2693(86)91377-8. URL: http://www.sciencedirect.com/science/article/pii/0370269386913778.

Huh, Ji-Haeng, Jihn E. Kim, Jong-Chul Park, et al. (June 2008). "Galactic 511 keV line from MeV millicharged dark matter". In: *Physical Review D* 77, 123503, p. 123503. DOI: 10.1103/PhysRevD.77.123503. arXiv: 0711.3528 [astro-ph].

Jedamzik, Karsten (Sept. 2004). "Did something decay, evaporate, or annihilate during big bang nucleosynthesis?" In: *Physical Review D* 70, 063524, p. 063524. DOI: 10.1103/PhysRevD.70.063524. arXiv: astro-ph/0402344 [astro-ph].

Jungman, Gerard, Marc Kamionkowski, and Kim Griest (1996). "Supersymmetric dark matter". In: *Physics Reports* 267.5, pp. 195–373. ISSN: 0370-1573. DOI: https://doi.org/10.1016/0370-1573(95)00058-5. URL: http://www.sciencedirect.com/science/article/pii/0370157395000585.

Kaplan, David E., Gordan Z. Krnjaic, Keith R. Rehermann, et al. (May 2010). "Atomic dark matter". In: *Journal of Cosmology and Astroparticle Physics* 2010, 021, p. 021. DOI: 10.1088/1475-7516/2010/05/021. arXiv: 0909.0753 [hep-ph].

Kaplinghat, Manoj, Sean Tulin, and Hai-Bo Yu (Feb. 2014). "Direct detection portals for self-interacting dark matter". In: *Physical Review D* 89, 035009, p. 035009. DOI: 10.1103/PhysRevD.89.035009. arXiv: 1310.7945 [hep-ph].

Kauffmann, G., S.D.M. White, and B. Guiderdoni (Sept. 1993). "The Formation and Evolution of Galaxies Within Merging Dark Matter Haloes". In: *Monthly Notices of the Royal Astronomical Society* 264, p. 201. DOI: 10.1093/mnras/264.1.201.

Klypin, Anatoly, Andrey V. Kravtsov, Octavio Valenzuela, et al. (Sept. 1999). "Where Are the Missing Galactic Satellites?" In: *The Astrophysical Journal* 522.1, pp. 82–92. DOI: 10.1086/307643. URL: https://doi.org/10.1086%2F307643.

Kolb, E.W. and M.S. Turner (1990). *The early universe*.

Kolb, Edward W., David Seckel, and Michael S. Turner (Apr. 1985). "The shadow world of superstring theories". In: *Nature* 314, pp. 415–419. DOI: 10.1038/314415a0. URL: https://doi.org/10.1038/314415a0.

Loeb, Abraham and Neal Weiner (Apr. 2011). "Cores in Dwarf Galaxies from Dark Matter with a Yukawa Potential". In: *Physical Review Letters* 106, 171302, p. 171302. DOI: 10.1103/PhysRevLett.106.171302. arXiv: 1011.6374 [astro-ph.CO].

Lynds, R. and V. Petrosian (Jan. 1989). "Luminous arcs in clusters of galaxies". In: *The Astrophysical Journal* 336, pp. 1–8. DOI: 10.1086/166989.

Macciò, A. V. and F. Fontanot (May 2010). "How cold is dark matter? Constraints from Milky Way satellites". In: *Monthly Notices of the Royal Astronomical Society* 404, pp. L16–L20. DOI: 10.1111/j.1745-3933.2010.00825.x. arXiv: 0910.2460.

MACHO Collaboration (Oct. 2000). "The MACHO Project: Microlensing Results from 5.7 Years of Large Magellanic Cloud Observations". In: *The Astrophysical Journal* 542, pp. 281–307. DOI: 10.1086/309512. arXiv: astro-ph/0001272 [astro-ph].

Markevitch, M., A. H. Gonzalez, D. Clowe, et al. (May 2004). "Direct Constraints on the Dark Matter Self-Interaction Cross Section from the Merging Galaxy Cluster 1E 0657-56". In: *The Astrophysical Journal* 606.2, pp. 819–824. DOI: 10.1086/383178. URL: https://doi.org/10.1086%2F383178.

Milgrom, M. (July 1983). "A modification of the Newtonian dynamics as a possible alternative to the hidden mass hypothesis". In: *The Astrophysical Journal* 270, pp. 365–370. DOI: 10.1086/161130.

Moore, Ben, Sebastiano Ghigna, Fabio Governato, et al. (Oct. 1999). "Dark Matter Substructure within Galactic Halos". In: *The Astrophysical Journal* 524.1, pp. L19–L22. DOI: 10.1086/312287. URL: https://doi.org/10.1086%2F312287.

Navarro, J. F., V. R. Eke, and C. S. Frenk (Dec. 1996). "The cores of dwarf galaxy haloes". In: *Monthly Notices of the Royal Astronomical Society* 283, pp. L72–L78. DOI: 10.1093/mnras/283.3.L72. eprint: astro-ph/9610187.

Navarro, Julio F., Carlos S. Frenk, and Simon D. M. White (Dec. 1997). "A Universal Density Profile from Hierarchical Clustering". In: *The Astrophysical Journal* 490.2, pp. 493–508. DOI: 10.1086/304888. URL: https://doi.org/10.1086%2F304888.

Okun, L. B. (Sept. 1982). "Limits on electrodynamics: paraphotons?" In: *Soviet Physics—JETP* 56.3, pp. 502–505.

Particle Data Group (Aug. 2018). "Review of Particle Physics". In: *Physical Review D* 98.3. ISSN: 2470-0010. DOI: 10.1103/PhysRevD.98.030001.

Planck Collaboration (July 2018). "Planck 2018 results. VI. Cosmological parameters". In: *arXiv e-prints*, arXiv:1807.06209. arXiv: 1807.06209 [astro-ph.CO].

Pontzen, Andrew and Fabio Governato (Apr. 2012). "How supernova feedback turns dark matter cusps into cores". In: *Monthly Notices of the Royal Astronomical Society* 421, pp. 3464–3471. DOI: 10.1111/j.1365-2966.2012.20571.x. arXiv: 1106.0499 [astro-ph.CO].

Pospelov, Maxim and Josef Pradler (Nov. 2010). "Metastable GeV-scale particles as a solution to the cosmological lithium problem". In: *Physical Review D* 82, 103514, p. 103514. DOI: 10.1103/PhysRevD.82.103514. arXiv: 1006.4172 [hep-ph].

Pospelov, Maxim, Adam Ritz, and Mikhail Voloshin (Apr. 2008). "Secluded WIMP dark matter". In: *Physics Letters B* 662, pp. 53–61. DOI: 10.1016/j.physletb.2008.02.052. arXiv: 0711.4866 [hep-ph].

Redondo, Javier (July 2008). "Helioscope bounds on hidden sector photons". In: *Journal of Cosmology and Astroparticle Physics* 2008, 008, p. 008. DOI: 10.1088/1475-7516/2008/07/008. arXiv: 0801.1527 [hep-ph].

Redondo, Javier and Marieke Postma (Feb. 2009). "Massive hidden photons as lukewarm dark matter". In: *Journal of Cosmology and Astroparticle Physics* 2009, 005, p. 005. DOI: 10.1088/1475-7516/2009/02/005. arXiv: 0811.0326 [hep-ph].

Reno, M. H. and D. Seckel (June 1988). "Primordial nucleosynthesis: The effects of injecting hadrons". In: *Physical Review D* 37 (12), pp. 3441–3462. DOI: 10.1103/PhysRevD.37.3441. URL: https://link.aps.org/doi/10.1103/PhysRevD.37.3441.

Roberts, M. S. and A. H. Rots (Aug. 1973). "Comparison of Rotation Curves of Different Galaxy Types". In: *Astronomy and Astrophysics* 26, pp. 483–485.

Rubin, V. C. and W. K. Ford Jr. (Feb. 1970). "Rotation of the Andromeda Nebula from a Spectroscopic Survey of Emission Regions". In: *The Astrophysical Journal* 159, p. 379. DOI: 10.1086/150317.

Rubin, V. C., W. K. Ford Jr., and N. Thonnard (June 1980). "Rotational properties of 21 Sc galaxies with a large range of luminosities and radii, from NGC 4605 (R = 4 kpc) to UGC 2885 (R = 122 kpc)". In: *The Astrophysical Journal* 238, pp. 471–487. DOI: 10.1086/158003.

Sawala, Till, Carlos S. Frenk, Azadeh Fattahi, et al. (Apr. 2016). "The APOSTLE simulations: solutions to the Local Group's cosmic puzzles". In: *Monthly Notices of the Royal Astronomical Society* 457, pp. 1931–1943. DOI: 10.1093/mnras/stw145. arXiv: 1511.01098 [astro-ph.GA].

Slatyer, Tracy R., Nikhil Padmanabhan, and Douglas P. Finkbeiner (Aug. 2009). "CMB constraints on WIMP annihilation: Energy absorption during the recombination epoch". In: *Physical Review D* 80, 043526, p. 043526. DOI: 10.1103/PhysRevD.80.043526. arXiv: 0906.1197 [astro-ph.CO].

Soucail, G., Y. Mellier, B. Fort, et al. (Feb. 1988). "The giant arc in A 370 – Spectroscopic evidence for gravitational lensing from a source at z = 0.724". In: *Astronomy and Astrophysics* 191, pp. L19–L21.

Spergel, David N. and Paul J. Steinhardt (Apr. 2000). "Observational Evidence for Self-Interacting Cold Dark Matter". In: *Physical Review Letters* 84, pp. 3760–3763. DOI: 10.1103/PhysRevLett.84.3760. arXiv: astro-ph/9909386 [astro-ph].

Springel, V., J. Wang, M. Vogelsberger, et al. (2008). "The Aquarius Project: the subhaloes of galactic haloes". In: *Monthly Notices of the Royal Astronomical Society* 391.4, pp. 1685–1711. DOI: 10.1111/j.1365-2966.2008.14066.x. eprint: https://onlinelibrary.wiley.com/doi/pdf/

10.1111/j.1365-2966.2008.14066.x. URL: https://onlinelibrary.wiley.com/doi/abs/10.1111/j.1365-2966.2008.14066.x.

Tucker, W. H., H. Tananbaum, and R. A. Remillard (May 1995). "A search for 'failed clusters' of galaxies". In: *The Astrophysical Journal* 444, pp. 532–547. DOI: 10.1086/175627.

Tyson, J. A., F. Valdes, and R. A. Wenk (Jan. 1990). "Detection of systematic gravitational lens galaxy image alignments – Mapping dark matter in galaxy clusters". In: *The Astrophysical Journal, Letters* 349, pp. L1–L4. DOI: 10.1086/185636.

Vogel, Hendrik and Javier Redondo (Feb. 2014). "Dark radiation constraints on minicharged particles in models with a hidden photon". In: *Journal of Cosmology and Astroparticle Physics* 2014, 029, p. 029. DOI: 10.1088/1475-7516/2014/02/029. arXiv: 1311.2600 [hep-ph].

Vogelsberger, Mark, Jesus Zavala, and Abraham Loeb (2012). "Subhaloes in self-interacting galactic dark matter haloes". In: *Monthly Notices of the Royal Astronomical Society* 423.4, pp. 3740–3752. DOI: 10.1111/j.1365-2966.2012.21182.x. eprint: https://onlinelibrary.wiley.com/doi/pdf/10.1111/j.1365-2966.2012.21182.x. URL: https://onlinelibrary.wiley.com/doi/abs/10.1111/j.1365-2966.2012.21182.x.

Walsh, D., R. F. Carswell, and R. J. Weymann (May 1979). "0957 + 561 A, B: twin quasistellar objects or gravitational lens?" In: *Nature* 279, pp. 381–384. DOI: 10.1038/279381a0. URL: https://doi.org/10.1038/279381a0.

Zhang, Le, Xuelei Chen, Marc Kamionkowski, et al. (Sept. 2007). "Constraints on radiative dark-matter decay from the cosmic microwave background". In: *Physical Review D* 76, 061301, p. 061301. DOI: 10.1103/PhysRevD.76.061301. arXiv: 0704.2444 [astro-ph].

Zwicky, F. (1933). "Die Rotverschiebung von extragalaktischen Nebeln". In: *Helvetica Physica Acta* 6, pp. 110–127.